Cell, Vol. 68, 33–51, January 10, 1992, Copyright © 1992 by Cell Press

Multipotent Neural Cell Lines Can Engraft and Participate in Development of Mouse Cerebellum

Evan Y. Snyder,*†‡ David L. Deitcher,* Christopher Walsh,*† Susan Arnold-Aldea,*§ Erika A. Hartwieg,‖ and Constance L. Cepko*
*Department of Genetics
†Department of Neurology
‡Department of Pediatrics
§Department of Obstetrics-Gynecology
Harvard Medical School
Boston, Massachusetts 02115
Department of Biology
‖Massachusetts Institute of Technology
Cambridge, Massachusetts 02139

Summary

Multipotent neural cell lines were generated via retrovirus-mediated v-*myc* transfer into murine cerebellar progenitor cells. When transplanted back into the cerebellum of newborn mice, these cells integrated into the cerebellum in a nontumorigenic, cytoarchitecturally appropriate manner. Cells from the same clonal line differentiated into neurons or glia in a manner appropriate to their site of engraftment. Engrafted cells, identified by *lacZ* expression and PCR-mediated detection of a unique sequence arrangement, could be identified in animals up to 22 months postengraftment. Electron microscopic and immunohistochemical analysis demonstrated that some engrafted cells were similar to host neurons and glia. Some transplant-derived neurons received appropriate synapses and formed normal intercellular contacts. These data indicate that generating immortalized cell lines for repair of, or transport of genes into, the CNS may be feasible. Such lines may also provide a model for commitment and differentiation of cerebellar progenitor cells.

Introduction

Little is known about the molecular and cellular mechanisms underlying development of the mammalian central nervous system (CNS). If one could study the properties of individual progenitors, perhaps by immortalizing such cells, it may be possible to unravel some of the complexities of cell-type determination and plasticity in the immature CNS. We (Ryder et al., 1990) and others (Fredericksen et al., 1988; Bartlett et al., 1988; Geller and Dubois-Dalcq, 1988; Evrard et al., 1990; Birren and Anderson, 1990) previously reported the establishment of immortalized clonal neural cell lines using retrovirus vectors to transduce oncogenes. Our lines were generated by retrovirus-mediated v-*myc* transfer into progenitors cultured from neonatal mouse cerebellum. Lines were established at a time when glia and neurons—the two major classes of cell type in the CNS—were being generated from the cerebellar external germinal layer (EGL). The EGL is a transient zone of small mitotic cells coating the external surface of the developing cerebellar cortex. Arising on embryonic day 13 by migration of cells from the fourth ventricle onto and over the external surface of the cerebellum, the EGL was viewed by classical neuroanatomists as a persistent primitive ventricular zone. It has often been used as a test tissue for hypotheses on histogenesis in the nervous system (Schaper, 1897; Miale and Sidman, 1961) owing, in part, to its relatively late development and accessibility. Present at birth in mammals, the EGL continues to proliferate postnatally, reaching a maximum 8-cell thickness at the end of the first postnatal week and disappearing by the end of the third postnatal week in rodents.

Our v-*myc*-immortalized cerebellar cell lines, established from the mouse EGL, evinced different morphologies and different cell type–specific antigens, even within a given clone. These results suggested that the original immortalized progenitor cells were multipotent, in keeping with results from in situ lineage analysis in a number of CNS locations (Turner and Cepko, 1987; Turner et al., 1990; Holt et al., 1988; Wetts and Fraser, 1988; Gray et al., 1988; Galileo et al., 1990; Leber et al., 1990). Not only was there diversity within clones, but lines were also observed to change during passage in vitro, alternating apparently spontaneously between predominantly neuronal and predominantly glial phenotypes. While changes in differentiation status may have simply reflected an instability in genome structure and/or expression, the heterogeneity and lability observed in vitro could in fact reflect the potential of progenitors in vivo in terms of their responsiveness to microenvironmental signals. To test whether the lines could respond appropriately when presented with the normal developmental cues of the cerebellar environment, as well as to probe the feasibility of using such lines for transduction of genes and/or functions into the in vivo environment, the lines were transplanted into the EGL of developing mouse cerebellum. The engrafted cells were then examined to determine whether they could participate in normal cerebellar development.

To identify the cell lines, they were marked by infection with a second retrovirus encoding the *lacZ* reporter gene (Price et al., 1987), the product of which forms a blue, electron-dense precipitate. During cerebellar histogenesis and at adulthood, the cerebella of transplant recipients were processed for identification of donor cells at the light and/or EM level. We now report that transplanted cells integrated into developing cerebellum in a nontumorigenic, cytoarchitecturally appropriate manner. Cells from the same clonal line differentiated into at least two neuronal types or into glia consistent with their site of engraftment. Derivation of engrafted cells from the clonal cell line was confirmed not only by its expression of the *lacZ* gene product but also, in some cases, by identity of the viral integration site between the donor cell line and labeled cells (portions of whose genome were amplified via the polymerase chain reaction [PCR]). Exogenous Escherichia coli β-galactosidase could be transduced and expressed within the cytoarchitectonics of the mammalian

CNS for prolonged periods, at least 22 months posttransplant. In a recent, independent study using a temperature-sensitive SV40 T antigen–immortalized hippocampal cell line, Renfranz et al. (1991) report engraftment and differentiation 3–6 weeks posttransplant.

The strategy of using retrovirus-immortalized lines as transduction agents for exogenous factors or as integral members of the cytoarchitecture of CNS tissue may be feasible for both clinical and research applications.

Results

Characteristics of Multipotent Neural Cell Lines prior to Transplantation

The establishment and in vitro characterization of these cerebellar progenitor cell lines has been detailed previously (Ryder et al., 1990). Briefly, retroviruses encoding v-*myc*, transcribed from the viral long terminal repeat (LTR) (plus the *neo* gene transcribed from an internal SV40 early promoter) were introduced into primary cultures of dissociated neonatal mouse cerebellum. Drug-resistant colonies were picked on the basis of morphology and passaged to establish separate lines that were then characterized using antisera to cell type–specific antigens.

Lines were established from G418-resistant colonies that exhibited different morphologies and that reacted with different cell type–specific antisera, suggesting either neuronal or glial lineages. However, some of these lines were found to have identical viral integration sites, suggesting that they derived from infection and immortalization of the same progenitor cell in the primary culture. For example, two lines that shared a common integration site, C17 and C36, were from the same primary culture and presumably derived from sibling cells that formed independent colonies upon initial expansion of the infected primary culture. Both colonies were selected because they contained cells that bore processes, an uncommon phenotype in the cultures. Though both colonies were process bearing, the morphology of the cells was different in the two, as was, on occasion, their antibody reactivity, suggesting that they might represent different cell types. Another line, C27, derived from an independent colony in the same culture, had a distinct integration site in addition to another distinct process-bearing morphology. Some lines thus could be categorized into clonally related "families" based on the location of their respective viral insertion sites. Nevertheless, all three of the above mentioned lines displayed similar qualities of neuronal–glial multipotency, heterogeneity, and lability. Periods of dual cell type–marker positivity or the transient expression of some markers was common, and antibody staining was rarely homogeneous. Subclones of all three lines were made and were found to exhibit these same properties.

As reported in Ryder et al. (1990), the two families of lines used in the following experiments (i.e., the C17/C36 family, the C27 family, and their respective subclones) each had the potential in vitro for expression of markers specific for oligodendrocytes (galactocerebroside C [Raff et al., 1978]) and neurons (neurofilament [NF; Wood and Anderton, 1981]). Subclones of C27 also expressed a marker for astrocytes (glial fibrillary acidic protein [GFAP; Bignami et al., 1972]). Subclones of the C17/36 family, generated for the transplantation experiments, also began to show expression of GFAP subsequent to publication of Ryder et al. (1990). When carried for prolonged periods in culture, some lines (e.g., C27 and C36) became dominated by cells of a flat, non-process-bearing morphology and lost the ability to stain for markers of differentiated cell types in culture.

To define further the similarity of the cerebellar lines to primary cerebellar tissue, C27-3, a subclone of C27 infected with the *lacZ*-encoding retrovirus BAG (Price et al., 1987), was reacted with a battery of antibodies reported to stain within cerebellum for defined cell types, both of neuronal and glial classifications. In addition to the previously mentioned markers, subsets of the same culture of C27-3 stained for the following markers: neuron-specific enolase, the neurotransmitter glutamate, and the monoclonal antibody Q600 (Gravel et al., 1987). All three of these antibodies are specific to neurons, primarily granule cells (GCs), when applied to the cerebellum; their reactivity with noncerebellar cells has not been defined. In addition, F41 (Smith et al., 1990, Soc. Neurosci., abstract), which is reactive with GCs and Purkinje cells, and Q111 (Gravel et al., 1987), which is reactive with cerebellar oligodendrocytes, showed positive staining. C27-3 also stained for microtubule-associated protein 1, a neuronal marker, and myelin basic protein, an oligodendrocyte-specific marker.

As a preliminary assessment of whether the lines were responsive to cues from bona fide cerebellar cells, an in vitro coculture experiment was performed. C17-2 and C27-3 were cocultured with primary dissociated cells from the newborn mouse cerebellum. They were then identified by X-gal histochemistry and evaluated for changes in growth properties and morphology. Both cerebellar lines stopped proliferating in the coculture and underwent dramatic alterations in mophology. When cultured alone, both lines were dominated by large, flat, epithelial-like cells (Figure 1A). In the presence of primary cerebellar cells, the soma of C27-3 and C17-2 became compact and small with long, usually bipolar but occasionally multipolar processes present on the majority of X-gal$^+$ cells (Figure 1B).

Integration into Developing Cerebellum

Cells from a given line were marked by infection in vitro with a replication-incompetent retroviral vector transducing the histochemically detectable E. coli *lacZ* gene (BAG virus) (Price et al., 1987). Subclones were picked, expanded, and tested for β-galactosidase expression, as detailed in the Experimental Procedures. Subclones that contained >90% β-gal$^+$ cells were further maintained. These were tested for the presence of helper virus and characterized immunocytochemically for cell type–specific markers prior to transplantation.

Approximately 2×10^4 to 6×10^4 cells of a given line were injected into the EGL of the cerebellum of newborn mice. Animals were sacrificed either during the first postnatal week (6 hr to 7 days posttransplant) when cerebellar histogenesis is active and the EGL is most prominent, or at

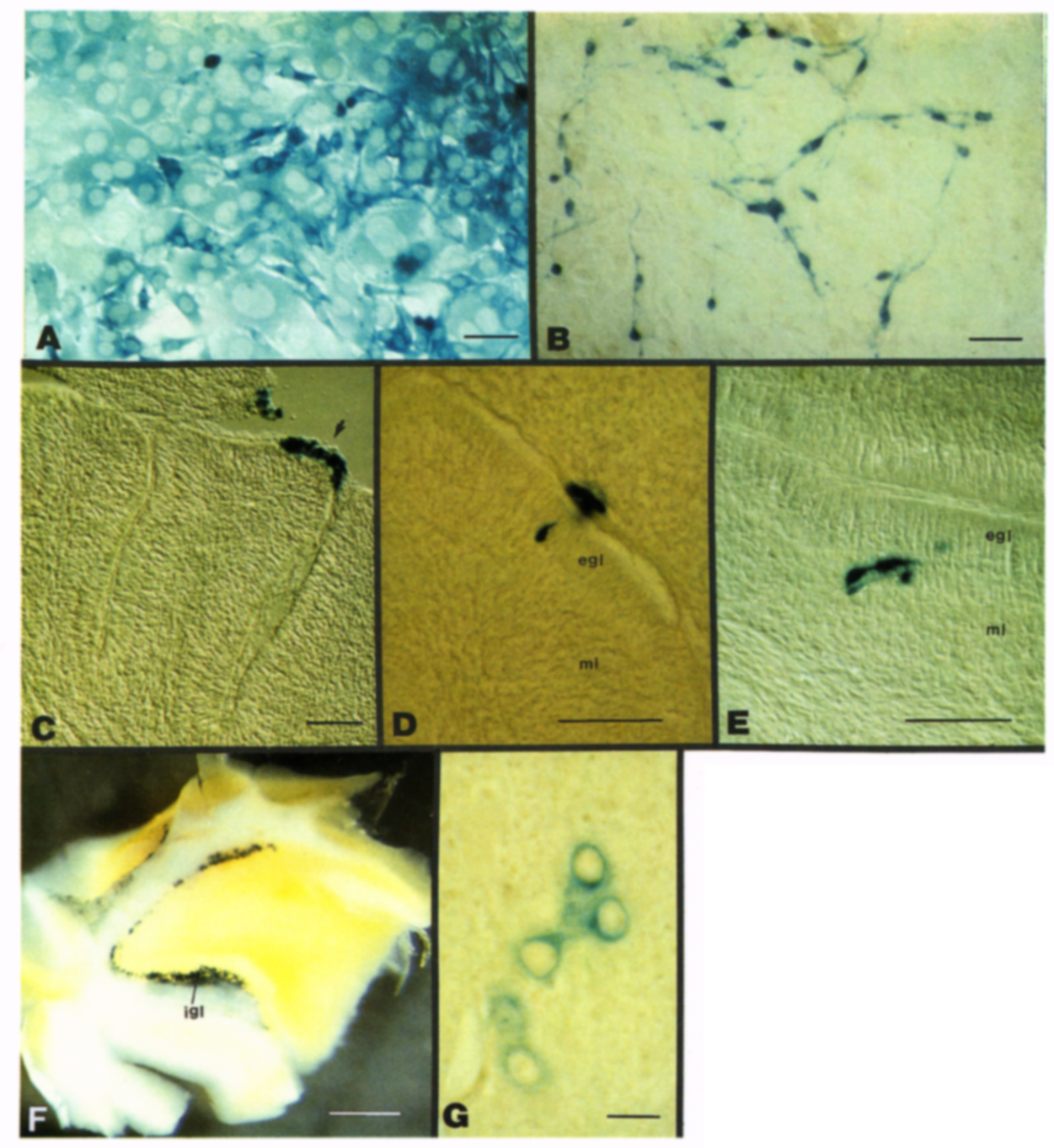

Figure 1. Cerebellar Cell Line C27-3 Can Respond to Environmental Cues In Vitro and Can Engraft into Developing Cerebellum

(A–B) Cerebellar cell line C27-3 cocultured with primary dissociated mouse cerebellum. After 8 days in vitro, C27-3 (blue, X-gal$^+$ cells) stopped proliferating and sent out processes in the cocultures (B) but not in the control, noncocultured wells (A).

(C–E) Cerebellar cell line transplants analyzed during cerebellar histogenesis. Parasagittal sections of cerebella from pups processed for *lacZ* expression during cerebellar histogenesis in the first week of life, shortly following transplantation of line C27-3. A relatively small number of cells actually apposed the EGL initially (6 hr posttransplant; [C], arrow), began integrating, and appeared to migrate (72 hr posttransplant; [D] and [E], respectively). Arrow in (C) indicates pial surface. (E) illustrates the typical spindle-shaped migratory pattern of a cell leaving the lower EGL and entering the nascent molecular layer (ml).

(F–G) Cerebellar cell line transplant, analyzed at adulthood. (F) shows dense incorporation of blue cells within the internal granular layer (igl) of the cerebellum from a 22 month old mouse who, as a newborn, received a transplant of line C27-3. The cerebellum as pictured in (F) was processed for *lacZ* histochemistry as an ~0.5 mm thick parasagittal floating section in preparation for electron microscopy. (G) shows a 1 μm semithin section of the IGL from the tissue pictured in (F). The blue histochemical precipitate created by the X-gal reaction formed a perinuclear ring around labeled transplanted cells.

Scale bars: (A) and (B), 50 μm; (C)–(E), 100 μm; (F), 500 μm; (G), 10 μm. Photographed using Nomarski optics in (A)–(E) and (G) and bright-field optics in (F).

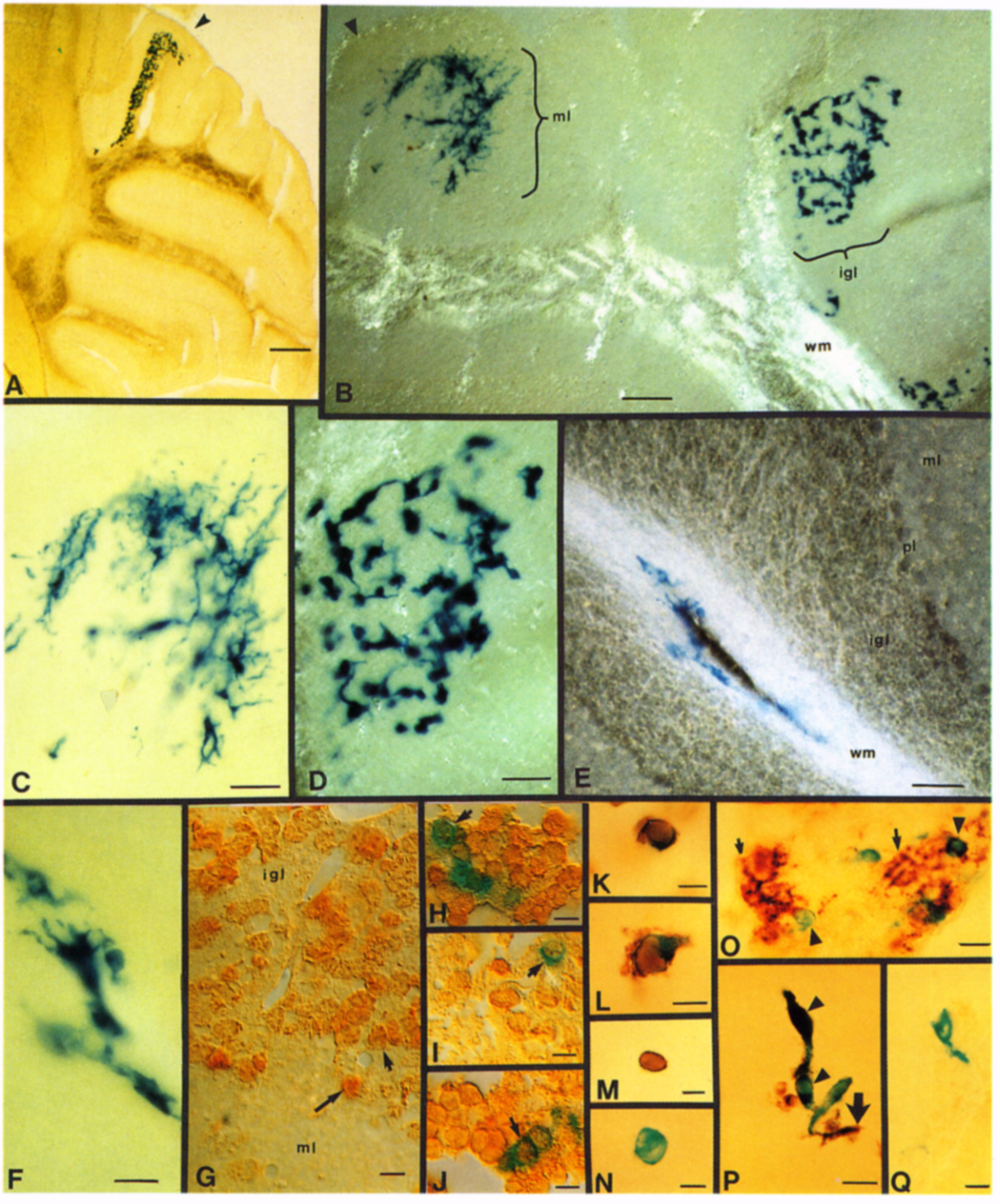

Figure 2. Differentiation of Cerebellar Lines into Neurons and Glia after Stable Engraftment into the Developing Cerebellum

(A) Cerebellar cell line transplant recipient, analyzed at adulthood. Blue cells occupying the IGL of the top-most folium (arrowhead) are cells from line C27-3 transplanted into a newborn mouse and visualized in this 60 μm thick parasagittal section of cerebellum by X-gal histochemistry at 8 months of age (arrowhead positioned at pial surface).

(B–D) Shown in (B) is a 60 μm section from the same cell line and same animal pictured in (A), ~1 mm away parasagittally. The group of X-gal$^+$ cells on the right of (B) are located in the IGL (layer closest to white matter tracts [wm]) and possess neuronal (GC) morphology, as seen at higher power in (D); the cells in the IGL of (A) also look like this at high power. The group of X-gal$^+$ cells on the left of (B) are primarily located in and virtually span the molecular layer (ml; farthest from wm) and possess glial (astrocytic) morphology, as seen at higher power in (C). Arrowhead in (B) indicates pial surface.

(E) X-gal$^+$ cells located along white matter tracts (wm) in a 30 μm section of adult cerebellum from another C27-3 transplant recipient.

(F) High power view of cells pictured in (E). This animal also contained X-gal$^+$ cells of the two types pictured in (B) (not shown). pl, Purkinje cell layer, a discontinuous, single layer of large cells oriented between the IGL and the ML.

adulthood (1–22 months of age), by which time cerebellar development and differentiation are complete. Sections of the cerebellum (either 60 μm cryostat sections affixed to gelatin-coated slides or 100–500 μm floating sections) were processed using X-gal histochemistry to locate labeled cells.

Analysis In First Week

Analysis of pups during the first week of life revealed engraftment of transplanted cells into the EGL, occasionally as early as 6 hr posttransplantation, but clearly by 72 hr. Between 3 and 7 days posttransplantation, engrafted cells in the EGL could often be seen assuming the spindle-shaped morphology previously described as indicative of migration of endogenous, newly postmitotic EGL-derived cells (Miale and Sidman, 1961; Smeyne and Goldowitz, 1989). The labeled cells appeared to migrate from the lower EGL into and across the molecular layer (ML) toward the widening internal granular layer (IGL), the layer where mature GC neurons reside. Of the large number of cells injected for transplantation, a relatively small number actually apposed the EGL initially (Figure 1C) (4.6% of the inoculum 6 hr posttransplant, averaged from two representative animals), and an even smaller number could be seen actually within the EGL and/or appearing to migrate from it (Figures 1D and 1E) (1.8% of the inoculum 72 hr posttransplant, averaged from two representative animals); most of the cells either immediately escaped along the injection tract out the injection hole, entered intermeningeal spaces, or became otherwise inaccessible to neural tissue for engraftment (not shown). Occasionally, large foci of cells were noted intraparenchymally, clearly deposited there by an excessively deep injection.

Analysis at Adulthood

Sections of cerebellum processed at adulthood revealed appropriate integration of labeled cells into that structure's cytoarchitecture with no evidence of tumor formation. In the animal pictured in Figure 2A, sacrificed at 8 months of age, $\sim 10^4$ cells from C27-3 spanning 1.7 mm (medial–lateral dimension) were incorporated. They were predominantly in the IGL and primarily in the vermis (subdivision of the cerebellum located in the midline) and posterior lobules. In the animal pictured in Figure 1F, sacrificed at 22 months of age, approximately twice as many cells (from C27-3) spanning twice that distance were detected.

Within the animal pictured in Figure 2B, some cells from C27-3 were located within the IGL and possessed neuronal morphology, suggestive of GCs (Figure 2D); other cells from that line were located within the ML and possessed glial morphology, suggestive of astrocytes (Figure 2C). Others from that line, e.g., in the animal pictured in Figures 2E and 2F, were found to reside along white matter tracts, assuming the location and morphology characteristic of a different glial cell type (oligodendrocytes). Multiple morphologies suggestive of multiple fates were observed in 5 adult animals transplanted with C27-3 and in 2 adult animals transplanted with C17-2. Further analysis of the nature of engrafted cells using ultrastructural and immunohistochemical criteria will be presented below. A fibroblast cell line expressing the *lacZ* gene, transplanted as a control, always failed to engraft.

Lack of Tumorigenicity

No tumors have ever been seen in more than 200 animals receiving transplants of various neural cell lines and various passages of those lines, often followed for more than 2 years posttransplant. Furthermore, animals with successful cerebellar transplants were never ataxic or otherwise motorically impaired.

Efficiency of Long-Term Engraftment

To date, there have been 34 animals in which X-gal$^+$ cells have been found within the cerebellum following transplantation (Table 1). Of these, 14 were present in adults; of these adult cerebella, 10 contained what appeared to be neurons (8 of these in combination with glia); 4 contained what appeared to be glia alone. The number of engrafted cells noted at adulthood varied widely, though attempts were always made to keep the initial inoculum constant in terms of concentration and amount across experiments (as described in the Experimental Procedures). There were many experiments (18) in which no engraftment was observed. In addition to the 34 positive animals presented in the Table 1, there were 172 animals in which no cerebellar engraftment was detected (16 pups, 156 adults).

Two out of three clonal lines examined (C17 and C27),

(G) Cerebellum stained with a cerebellar neuronal nuclear marker. A paraffin-embedded section of cerebellum (1 μm thick) was reacted with the cerebellar neuronal nuclear antibody Q502 (courtesy of R. Hawkes) and visualized at high power. Neuronal nuclei are stained. The staining is located principally in the IGL, where GCs (e.g., short arrow) are abundant, is seen in the Purkinje cell layer (long arrow), and is virtually nonexistent in the ML, where neurons are sparse.

(H–J) Dual staining for β-galactosidase and the Q502 cerebellar neuronal nuclear marker. Three 1 μm thick paraffin-embedded sections from the IGL of the C27-3 transplant recipient pictured in Figures 1F and 1G reacted with Q502 as in (G). When immunoperoxidase staining followed X-gal processing, these double-labeled cells (arrows) had a brown bull's eye appearance within a blue perinuclear ring. Nuclei of endogenous GCs also exhibited the brown antibody stain but did not have the blue perinuclear precipitate.

(K–N) Shown are GC neurons mechanically dissociated and visualized as isolated individual cells following X-gal and/or immunocytochemical processing of 1 μm paraffin-embedded sections. (K) and (L) show double-labeled transplant-derived GC neurons from a recipient of C17-2 with blue perinuclear ring and brown bull's eye appearance following reaction with Q502 (alkaline phosphatase–conjugated secondary antibody). (M) illustrates endogenous GC exhibiting brown Q502 antibody stain but without the blue perinuclear precipitate. (N) shows negative control: an endogenous GC cell stained with an irrelevant antibody.

(O–Q) Transplant-derived cells from the ML stained for the glial (astrocytic) marker GFAP. In (O), cells from the ML of the C17–2 transplant recipient studied in (K) and (L) were stained in situ for GFAP as per (H)–(J). Robust staining was noted, primarily of processes (arrows) and occasionally of cell bodies (arrowhead). In (P), blue cells from ML of this animal mechanically dissociated as per (K)–(N) following GFAP staining. Arrowhead indicates GFAP-labeled brown-blue cell bodies. Arrow indicates anti-GFAP-labeled brown process that appeared to emanate from a blue cell. (Q) shows a negative control: transplant-derived GC from the same animal as in (K), (L), (O), and (P) stained instead for the glial marker GFAP.

Scale bars: (A), 300 μm; (B) and (E), 100 μm; (C) and (D), 50 μm; (F), 20 μm; (G)–(O) and (Q), 5 μm; (P), 25 μm. Photographed using Nomarski optics in (B), (D), and (G)–(J); bright-field optics in (A), (C), (F), and (K)–(Q); and dark-field optics in (E).

Table 1. Cell Line Transplant Recipients with Successful Engraftment in Cerebellum

Cell Line[a]	Age at Analysis[b]	Approximate Number of Cells Engrafted[c]	Efficiency of Experiment[d]	Neurons	Glia	EGL/ML[e]
C27-3[f]	22 months	4+	2/4	x[g,h]	x	
C27-3[f]	8 months	4+	2/4	x[g]	x	
C27-3[f]	3 months	2+	5/12	x	x	
C27-3	1.25 months	2+	1/5	x	x	
C17-2	2.7 months	3+	2/3	x[g]	x	
C17-2	2.7 months	4+	2/3	x[g]	x	
C27-3	1.5 months	2+	1/1	x	x	
C17-2	8.25 months	1+	1/4	x		
C17-2	3.5 months	1+	3/4	x		
C27-3	1.25 months	1+	1/3		x	
C27-3	1.25 months	1+	1/6		x	
C27-3	1.25 months	1+	1/6		x	
C36-4	8 months	1+	1/5	x	x	
C27-16	2.3 months	1+	3/3		x	
C27-3	P3	1+	5/12			x
C27-3	P3	1+	5/12			x
C27-3	P7	2+	5/12			x
C27-3	P7	2+	5/12			x
C27-3	P6	2+	1/14			x
C27-3	P6	2+	1/5			x
C27-3	P6	1+	1/2			x
C27-3	P4	2+	1/3			x
C27	P6	2+	1/1			x
C27	P4	1+	1/6			x
C27	P4	1+	2/4			x
C27	P14	2+	2/4			x
C27-11	P7	2+	1/7			x
C27-16	P7	2+	3/3			x
C27-16	P7	2+	3/3			x
C27-5	P3	1+	3/9			x
C27-5	P3	1+	3/9			x
C27-5	P7	1+	3/9			x
C17-2	P8	2+	3/4			x
C17-2	P8	2+	3/4			x

[a] A given cell line is designated by the number following "C", e.g., C27; a number following a dash refers to a subclone of that cell line, e.g., C27-3.
[b] Animals less than 1 month of age (adulthood) are designated by postnatal day of life (e.g., "P3") where day of birth = PO.
[c] Approximate number of *lacZ*$^+$ cells found at the indicated harvest date: 4+ = $>10^4$; 3+ = 10^3–10^4; 2+ = 10^2–10^3; 1+ = $<10^2$.
[d] Efficiency of engraftment in the particular experiment of which this animal was a member; numerator = number of positive animals in that experiment; denominator = total number of animals analyzed in that experiment.
[e] EGL = external germinal layer; ML = molecular layer (see text for details.).
[f] Confirmation that the viral insert in blue cells from a transplant recipient brain is identical to that of the donor cell line.
[g] Confirmed by electron microscopic evaluation of ultrastructure.
[h] Synapses on transplant-derived granule cell neurons identified by electron microscopy.

have shown multiple instances of engraftment. Of these, the respective subclones, C17-2 and C27-3, have proven the most successful and are therefore the best studied. However, the efficiencies vary greatly and, at present, inexplicably. They range from 0%–100% per experiment for the former (mean: 16%) and 25%–75% per experiment for the latter (mean: 55%), failure to engraft being the most common overall outcome at this point. However, since engraftment has been scored by expression of β-galactosidase, it is possible that engraftment rates are much higher, but that frequency of detectable β-galactosidase expression is significantly lower than the actual engraftment rate (see Discussion).

It should be noted that not all cell lines—even subclones of the same line—engraft (although given the low frequency of success with even the best lines, lack of engraftment by any line must be interpreted with caution). Furthermore, not all passages of even a competent line (e.g., C27-3) engraft with equal efficiency. We have not yet been able to determine which variables insure the greatest number of engrafted cells per animal with the greatest efficiency per litter. While the precise "engraftability" factor(s) remains elusive, it appears that periods during which the lines are process bearing in culture and display some percentage of differentiated neural markers (NF and/or GFAP) correlate with more reliable engraftment, as opposed to a flat morphology with no cell marker expression. While uniformly flat, non-marker-expressing cells almost never engraft, the converse, i.e., expression of markers, does not necessarily insure engraftment. The first 24–48 hr of life appeared the most "engraftable" age for a recipient newborn mouse pup; while efficiency of engraftment

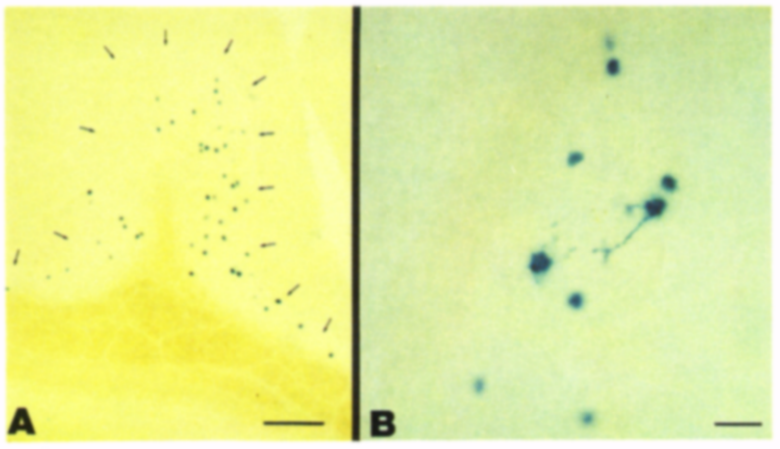

Figure 3. Distribution and Morphology of Host Cerebellar Cells after Transduction of the *lacZ* Gene

To generate X-gal-labeled host cerebellar cells for comparison with X-gal-labeled engrafted cells, neonatal mouse cerebellum of a nonengrafted host was infected by an injection of the BAG virus; the cerebellum was processed for X-gal histochemistry at adulthood.

(A) X-gal$^+$ host cells in parasagittal section of adult cerebellum are located primarily in the IGL (borders outlined by small arrows; pial surface is at the top of the photomicrograph). Compare with engrafted C27-3 X-gal$^+$ cells in Figure 2A.

(B) Higher power view of X-gal$^+$ host cells from cerebellum pictured in (A). Compare with engrafted X-gal$^+$ C27-3 cells in Figure 2D.

Scale bars: (A), 100 μm; (B), 20 μm. Photographed using bright-field optics in (A) and (B).

was only slightly better (18% at <P2 vs. 15% at ≤P2), there tended to be a larger number of engrafted cells seen in positive animals transplanted at the younger age.

Endogenous Granule Cells Observed In Situ

To compare the morphology and distribution of cells derived from transplanted lines with those derived from endogenous cerebellar progenitors, the BAG vector was injected directly into neonatal mouse cerebellum, labeling endogenous mitotic progenitors and their progeny in situ. After the cerebella were fully differentiated, sections of the tissue were processed to locate the marked cells. Blue cells were located principally in the IGL, consistent with their having been born postnatally in the EGL and having descended to terminate in the IGL (Figure 3A). Cell bodies were small and round with a few fine dendritic processes barely filled with the blue precipitate (Figure 3B). In contrast, the processes and cytoplasm of IGL cells derived from transplants were "plumper" and better defined (compare Figure 3B with Figure 2D). Parallel fibers of endogenous GCs, the axonal projections that form the ML, were never observed to be labeled by precipitate. Similarly, transplant-derived IGL cells did not exhibit labeled projections. This finding is not unexpected, as the X-gal precipitate has frequently failed to fill the processes of infected neurons and/or glia.

Although newly born GCs migrate from EGL to IGL down columns along radial glial fibers (Rakic, 1971), blue cells derived from either the cell lines or endogenous progenitors were seen not to be columnarly arrayed at adulthood, and cells in columns were far from uniformly blue. Rather, there was enormous scatter of blue cells derived from endogenous progenitors (Figure 3A). A more clustered but still nonradial pattern of distribution of cells derived from the cell lines was seen. Occasionally, from either endogenous progenitors or from transplanted cells, different cell types (e.g., glia and neurons) were juxtaposed. Although a significant percentage of the endogenously derived labeled cells were no doubt clonally related, the extensive migration of labeled cells made it impossible to delineate clonal boundaries reliably.

Immunohistochemical Analysis of Engrafted Cells

Returning to examination of transplanted, exogenous cells, as shown in Figures 1 and 2, several morphologies and locations consistent with a variety of cell types were observed among stably engrafted cells. To characterize further the engrafted cells, antibodies directed against neuronal and glia cell types were used to stain X-gal$^+$ cells. When applied to tissue sections containing X-gal$^+$ cells, this approach was slightly hampered by the arrangement of cells within the adult cerebellum. For example, the IGL is an area of extremely high GC density. It is thus difficult to assess reliably whether X-gal$^+$ cells are positive or negative for a GC antigen, owing to the high endogenous antigen density. To circumvent this problem partially, two approaches were taken. Cryostat sections (60 μm) containing X-gal$^+$ cells were embedded in paraffin so that thinner, 1 μm sections, could be made. As the diameter of a GC is 5–8 μm, 1 μm sections partially relieved the problem of superposition of endogenous and transplant-derived cells. Second, after immunohistochemical processing of the section, cells within the section were mechanically disassociated. Individual cells could then be scrutinized.

Antibodies that react with cerebellar neurons were directed against the IGL from X-gal-processed tissue of transplant recipients, including those pictured in Figures 1F, 1G, and 2D. As in the semithin sections for electron microscopic (EM) analysis (Figure 1G), the perinuclear ring of the *lacZ* reaction product within the labeled cell left a clear nucleus; a nuclear anti-neuronal monoclonal antibody, detected with a conjugate of horseradish peroxidase or alkaline phosphatase, could be directed against such a cell, conferring a "bull's eye" appearance if successfully double labeled. The monoclonal antibody Q502, when directed against paraffin-embedded 1 μm sections of mouse cerebellum, stained most neuronal nuclei in the IGL (Figure 2G), as previously reported (Gravel et al.,

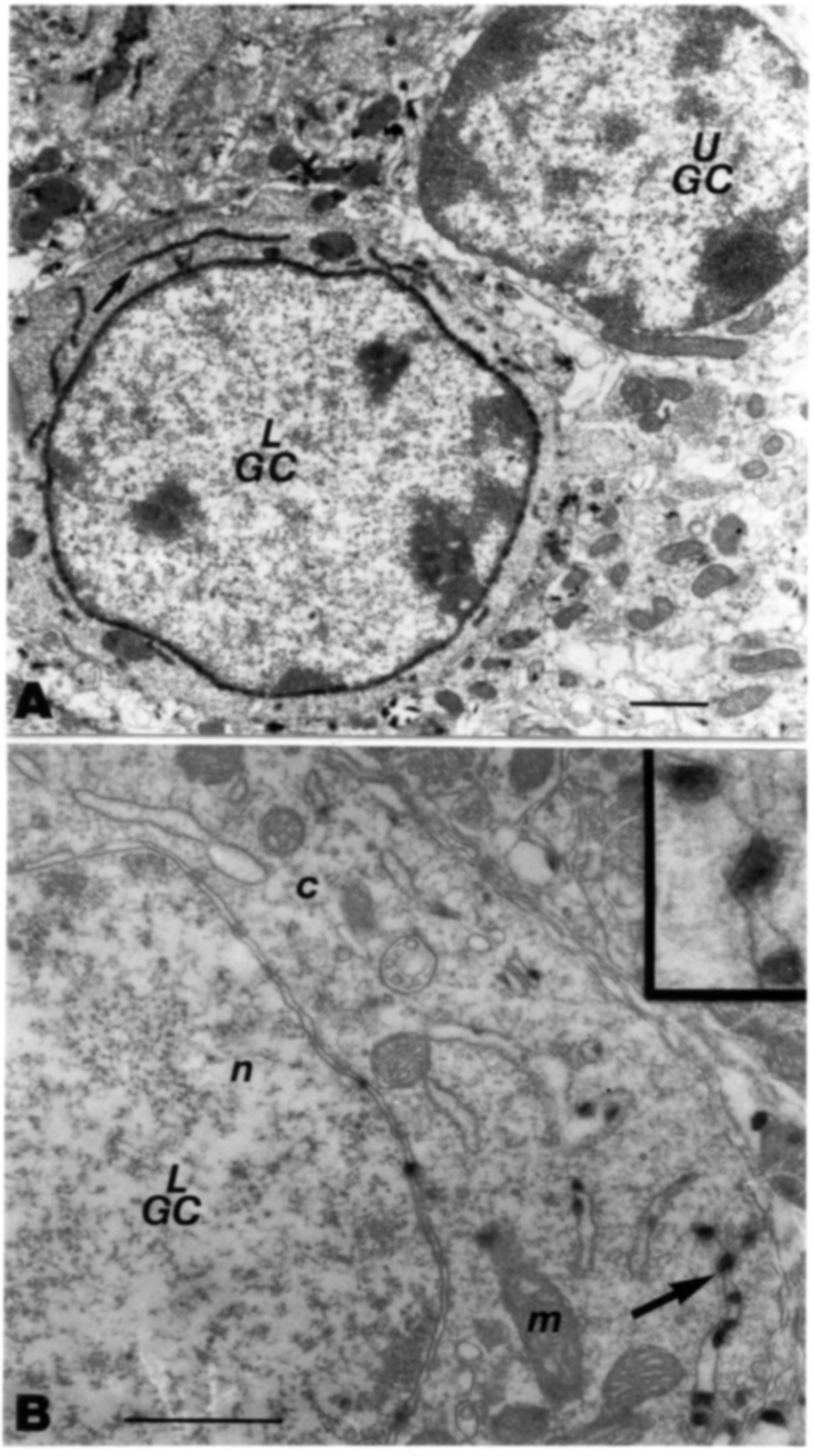
U
GC
L
GC
A
c
n
L
GC
m
B

1987). Cells within the IGL varied in their intensity of staining, and it appeared that cells within the Purkinje cell layer stained most intensely. Blue cells in the IGL of recipient animals, examined in this fashion, also stained positively with Q502 (Figures 2H–2J); they stained with a variety of intensities, some definitively positive (e.g., Figure 2J), and some less so (e.g., Figure 2I). Dissociated blue cells revealed brown nuclear staining (Figures 2K and 2L) similar to that of isolated endogenous GCs (Figure 2M), but distinguishable from blue GCs stained with an irrelevant antibody (Figure 2N) or with an antibody directed against the astrocyte marker GFAP (Figure 2Q).

A similar procedure using anti-GFAP antibody was performed for transplant-derived cells with glial morphology in the ML. Anti-GFAP stained blue cells in the ML in situ (Figure 2O) in a manner similar to that of endogenous cells (not shown). When the tissue was mechanically dissociated, staining of GFAP on individual blue cells was detectable and resembled staining of dissociated endogenous astrocytes (Figure 2P). The cell body, as well as processes, of some blue cells exhibited colocalization of the GFAP and X-gal stains. As previously noted, GFAP did not stain presumptive GCs, which stained for Q502 (Figure 2Q).

Ultrastructural Analysis

As the cerebellum has been extensively characterized at the ultrastructural level using electron microscopy, an assessment of the differentiation state (and thus functional potential) of engrafted cells is most reliably made using these criteria. Ultrastructural features also reliably confirm cell type identification (Palay and Chan-Palay, 1974).

Four positive recipient mouse cerebella were prepared for EM examination (Table 1). Floating sections (100–500 μm thick) of cerebella at adulthood were processed for X-gal histochemistry (Figure 1F). As seen in 1 μm semithin sections of the IGL (Figure 1G), the most obvious location of the blue histochemical precipitate created by dimerization of the X-gal product is in the perinuclear region of transplanted cells, distinguishing them from endogenous GC neurons. This precipitate is electron dense (Bonnerot et al., 1987), allowing engrafted labeled cells to be distinguished from endogenous GC, which they otherwise resemble ultrastructurally (Figure 4A). The precipitate is localized not only to the nuclear membrane but also to cytoplasmic, subcellular organelles such as the endoplasmic reticulum (ER) (Figures 4A and 4B, arrows). Individual particles, when examined under high power, appear crystalline (Figure 4B, inset).

GC neurons are identified ultrastructurally as small round or oval cells (5–8 μm diameter) in the IGL with meager cytoplasm forming a rim around a large round nucleus. The cytoplasm contains few mitochondria and short tubules of ER, sometimes squeezed into a small space within the cytoplasm created by dimpling of the nucleus. The nucleus contains large blocks of condensed chromatin usually distributed along the inner side of the nuclear envelope forming a characteristic "clock face appearance"; a small nucleolus is usually hidden within one of these chromatin blocks (Eccles et al., 1967; Palay and Chan-Palay, 1974; Peters et al., 1991; S. Palay, personal communication).

A second type of labeled, transplant-derived neuron was also identified, the basket cell (BC) neuron (Figures 5A and 5B). BCs are also born in the postnatal period, although their origin is somewhat controversial (Eccles et al., 1967; Altman, 1982; Miale and Sidman, 1961; Palay and Chan-Palay, 1974; Hallonet et al., 1990). In the normal cerebellum, BCs are very few in number, comprising 20-fold fewer cells than the extremely abundant GCs, and thus were seen labeled only rarely. BCs are defined ultrastructurally as larger cells (12–20 μm diameter) in the lower ML with ample cytoplasm and a distinctive large, indented (often deeply) irregular nucleus with dispersed, nonaggregated, less dense chromatin. The prominent ER cisternae are roughly parallel with the nuclear envelope (Eccles et al., 1967; Palay and Chan-Palay, 1974; S. Palay, E. Mugnaini, personal communication). As in the transplant-derived GCs, label was located within the nuclear envelope and in the ER.

Glial cells with label were also identified (Figures 5C–5E). One type of glial cell, an oligodendrocyte (Figures 5C and 5E), though somewhat similar in size and shape to a GC neuron, is identified by its distinctively dark cytoplasm, an appearance created in the mature cell by numerous fine granules. Because the nucleus lies somewhat eccentrically, a large mass of cytoplasm, while not voluminous, may occur at the poles of the cell. The contour of the perikaryon is smooth and regular. Unlike in the GC, the nuclear chromatin tends to marginate and flatten against the nuclear membrane and/or clump centrally, allowing a prominent nucleolus to be visualized in IGL oligodendrocytes. The mitochondria are short and round and the ER are usually well developed, long, meandering, and distended. Oligodendrocytes are usually located near myelinated fibers or near blood vessels (Palay and Chan-Palay, 1974; Peters et al., 1991). In Figure 5C, precipitate was seen in the nuclear membrane and ER of an ultrastructurally identified oligodendrocyte.

Evidence for label within a second type of glial cell, an

Figure 4. Engrafted Cells, Identified by Electron-Dense X-Gal Precipitate, Resemble Host Granule Cells at the Ultrastructural Level

Electron micrographs from the IGL of the C27-3 transplant recipient pictured in Figures 1F and 1G, 22 months posttransplant.

(A) The blue perinuclear histochemical precipitate is electron dense, allowing engrafted labeled cells (LGC) to be distinguished from endogenous unlabeled granule cell neurons (UGC), which they otherwise resemble ultrastructurally. Compare with light microscopic picture of a semithin section from a similar field in Figure 1G. The precipitate is localized in cytoplasmic, subcellular organelles (arrow)—the ER. Scale bar, 1 μm.

(B) A transplant-derived, labeled granule cell (LGC) in which the precipitate forms a discontinuous, more discrete pattern around the nucleus and in subcellular organelles (arrow). n, nucleus; c, cytoplasm; m, mitochondrion. Scale bar, 1 μm.

(B, inset) The three precipitate particles at the tip of the arrow in (B) are enlarged in order to demonstrate their crystalline character.

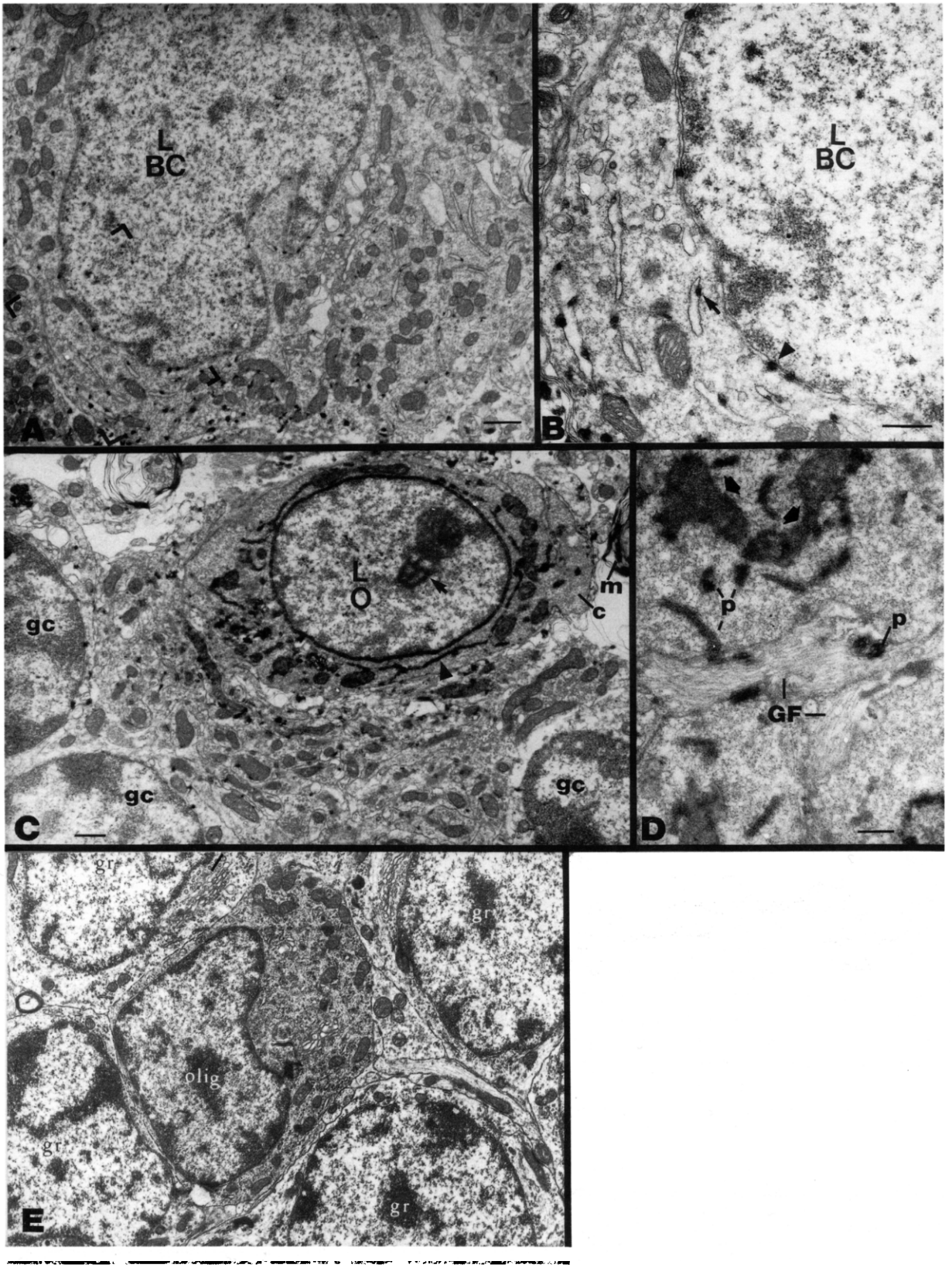

Figure 5. Engrafted Cells Resemble the Host BCs and Two Types of Glia at the Ultrastructural Level

(A) and (B) show a labeled basket cell neuron.

(A) Labeled BC neuron (LBC) in the lower ML displays defining ultrastructural features listed in the text, most prominently the deeply clefted nucleus and the ER coursing roughly parallel to the nuclear membrane. Label precipitate is seen in the nuclear membrane and in the ER. Scale bar, 1 μm.

(B) Blocked area in (A) at higher power. Note the label within the nuclear envelope (arrowhead) and adherent to the ER (arrow). Scale bar, 0.5 μm.

astrocyte, was also noted. Mature astrocytes are defined ultrastructurally by the presence of glial filaments (GFs) (the main constituent of which is defined by GFAP antibodies) (Palay and Chan-Palay, 1974; Peters et al., 1991; Bignami et al., 1972). Figure 5D demonstrates precipitate-bearing processes with GFs, defining them as astrocytic. GFs are defined and distinguished ultrastructurally from neurofilaments (NFs) by several criteria. In appearance, GFs are fine, smooth, uniform in size, closely packed, and unmyelinated. In contrast, NFs are coarse, "bumpy," of multiple sizes, widely spaced, loosely bundled, and often myelinated. GFs and NFs are also distinguished by their size. The labeled GFs (Figure 5D) measured on average 8.4 nm in width, appropriately ~76% of the diameter of NFs (Peters et al., 1991) in the same field.

The synaptic unit in the IGL is the glomerulus: incoming large, mossy fibers synapse on small dendrites from multiple GC neurons. When sliced transversely, as in an EM section, dendrites usually look like small, occasionally elongated, ovals containing a single mitochondrion and often a single ER vacuole, around which a mossy fiber envelops (Eccles et al., 1967; Palay and Chan-Palay, 1974). Figure 6A, obtained from the cerebellum pictured in Figures 1F and 1G, offers a low powered electron micrograph of a labeled, transplant-derived GC neuron (LGC). Near it (blocked area) are a number of synapses, indicated by arrows in the higher power overview of that region (Figure 6B). Further magnification of the blocked areas in Figure 6B (Figures 6C and 6D) demonstrate oval GC dendrites (gd) with label precipitate (p), which, as in the cell bodies, respects membrane boundaries (compare with Figure 4B, inset). Endogenous, unlabeled, multi-vesicle-filled mossy fibers (mf) synapse on them (arrows). The GC dendrites also make adhesive contacts ("puncta adherentia") (Figure 6C, arrowheads) (Palay and Chan-Palay, 1974) with other GC dendrites. Evidence of synapse formation was seen in several other areas within this engrafted animal.

Identity of Proviral Integration Site

Up to this point, identification of donor cells was by virtue of the X-gal histochemical reaction. Escape of the BAG genome from donor cells or contamination of the mice with BAG virus derived from any source could lead to infection of endogenous host cells and subsequent misidentification of host cells as donor cells. Therefore, several steps were taken to confirm that the X-gal$^+$ cells were donor derived. First, multiple tests for production of BAG virus by the donor cells were negative in all lines used for transplantation. Second, we sought to identify a unique genetic tag for donor cells that would allow confirmation that the blue cells within a recipient cerebellum were indeed donor derived. This was done by recovery of the sequence at the viral integration site in cell line C27-3 by an inverse PCR (see Experimental Procedures). Oligonucleotides complementary to stretches of sequence constituting the integration site were synthesized to serve as primers in direct PCR against opposing primers within the LTR. When the reaction was performed on genomic DNA from the C27-3 cell line, fragments of predicted size were obtained using all possible primer pairs. These products were specific for C27-3; amplification products were not obtained using genomic DNA from non–clonally related, BAG-infected cell lines generated from the same primary culture that generated C27-3. From the three recipient cerebella pictured in Figures 1G, 2A–2D, and 2E–2F, multiple pieces of tissue, each containing 1–20 blue cells, were dissected from diverse regions, digested with proteinase K, and subjected to PCR. When the amplification products were examined by electrophoresis, tissue containing blue cells yielded fragments of the predicted size, identical to that from the C27-3 cell line. Ninety percent of samples containing blue cells (27/30) successfully amplified. The 10% of samples that failed to amplify (3/30) contained only 1 blue cell each. Samples containing only 1 blue cell amplified 57% of the time (4/7), an efficiency in keeping with that observed for single BAG-infected cells dissected from rodent cortex (C. Walsh and C. L. Cepko, unpublished data). Lanes that contained either no tissue, cerebellar tissue from a littermate in which engraftment failed (i.e., no blue cells), or tissue from an uninjected cerebellum usually demonstrated no amplification product (Figure 7). The rare falsely positive samples (2/24 or 8.3%) presumably resulted from cross-contamination, a common finding when high cycle numbers are used in PCR.

Discussion

Stable Engraftment of Retrovirally Immortalized Lines

A number of studies recently have demonstrated that transplanted primary neural tissue, usually of fetal origin, can become successfully engrafted in host parenchyma (reviewed in Gage and Fisher, 1991). Some of these studies have addressed developmental questions—e.g., do grafted cells follow an autonomous program or do they accommodate to their new surroundings (Sotelo and Alvarado-Mallart, 1986, 1987; McConnell, 1985, 1988;

(C) Labeled glial cell (oligodendrocyte). Labeled oligodendrocyte (LO) present in the IGL displays the defining ultrastructural features that distinguish it from nearby granule cell neurons (gc) (see text). Specifically, there is a distinctively dark cytoplasm (c) that collects at the poles of the cell, a dark nucleus, a prominent nucleolus located near centrally clumped chromatin (arrow) with the remainder of the chromatin marginated as a rim along the inner nuclear membrane. Label is present in the nuclear membrane and in the long meandering ER (arrowhead). The cell is adjacent to a myelinated fiber (m). Scale bar, 1 μm. Compare with (E). olig, oligodendrocyte; gr, granule cell.

(D) Labeled glial (astrocytic) process containing GFs. A process bearing label precipitate (p) also contains GFs, which define that process as glial (astrocytic). (The process lies adjacent to the cytoplasm of labeled glial cells that border it on both sides and that themselves contain precipitate in ER and near poorly fixed mitochondria.) The GFs average 8.4 nm in diameter. Their distinctive appearance and size are discussed in the text.

(E) For comparison with (C), an endogenous IGL oligodendrocyte and granule cell are reproduced (with permission) from the textbook of Palay and Chan-Palay (1974) (their Figure 266).

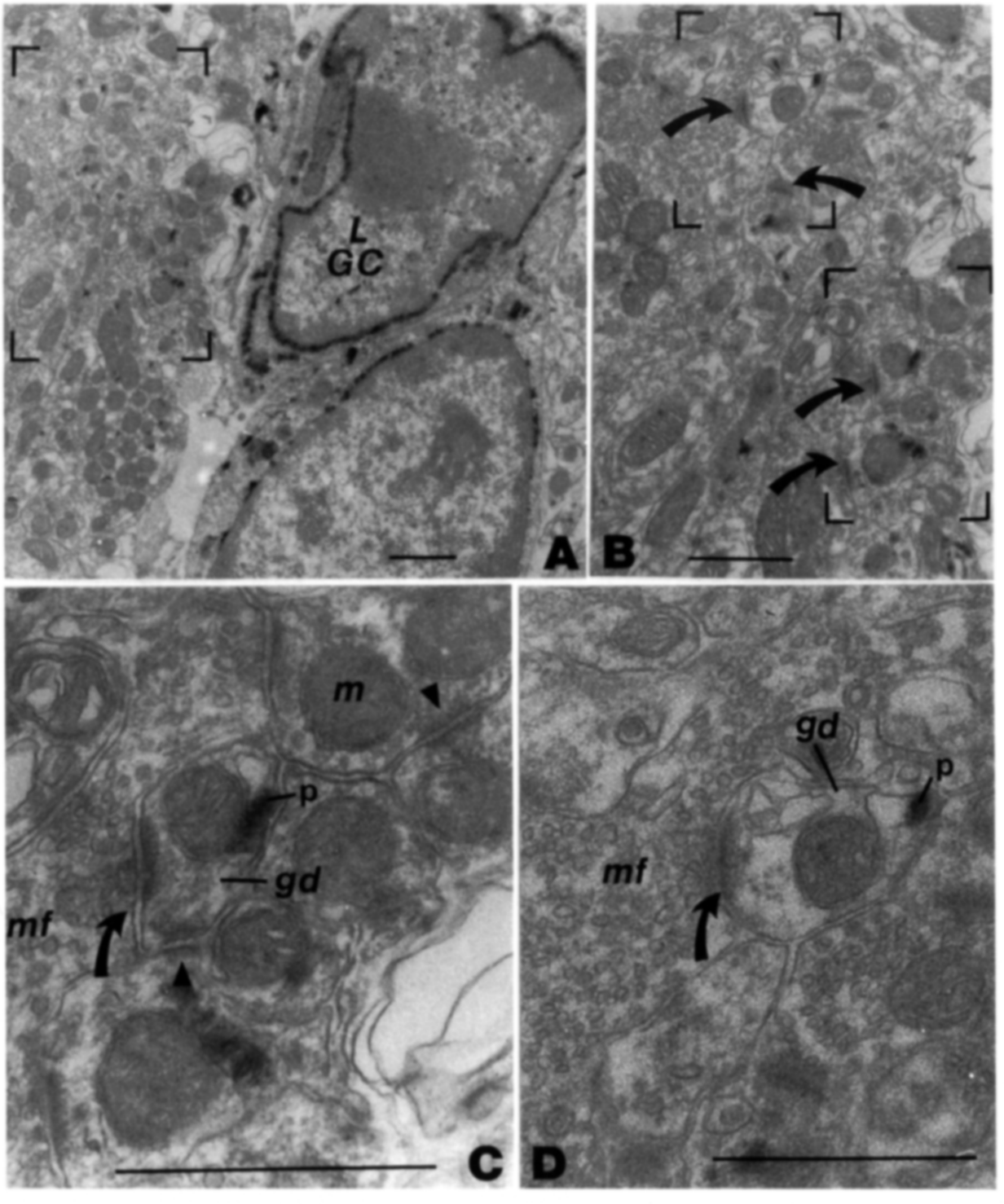

Figure 6. Postsynaptic Specializations on Labeled GC Dendrites

Electron micrograph from the IGL of the C27-3 transplant recipient pictured in Figures 1F, 1G, 4, and 5, 22 months posttransplant.

(A) Low power view of a transplant-derived, labeled granule cell neuron (LGC). Scale bar, 1 μm. Glomerular complexes near it (blocked area) are examined at higher power in (B) (scale bar, 1 μm), where arrows indicate a number of synapses. The blocked areas in (B) are further magnified in (C) (scale bar, 1 μm; lower block) and (D) (scale bar, 1 μm; upper block). Both (C) and (D) demonstrate oval granule cell dendrites (gd) with label precipitate (p). Note: the label respects membranes and resembles the precipitate in the GC bodies as seen under high power in Figure 4B, inset. Endogenous, unlabeled, multi-vesicle-filled mossy fibers (mf) synapse on the labeled granule cell dendrites (arrow). In (C), the GC dendrite also makes adhesive contacts (puncta adherentia) (arrowheads) with other granule cell dendrites. m, mitochondrion. See text for further explanation and definitions.

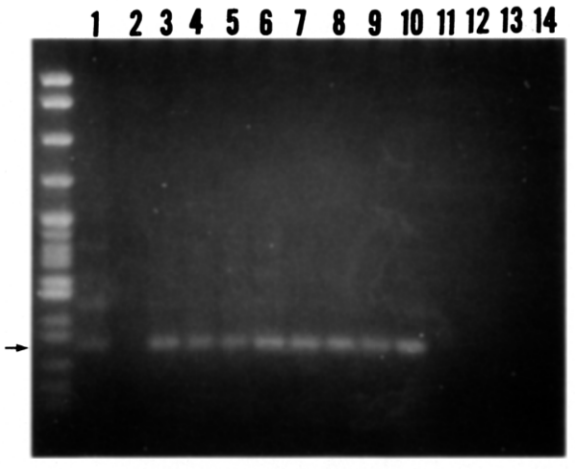

Figure 7. Blue Cells within a Recipient Cerebellum Bear the Same "Genetic Tag" As the Donor Cells

As detailed in the text, oligonucleotides complementary to portions of flanking sequence served as one-half of a set of primers for a PCR against opposing primers within the LTR. This gel shows the amplification products obtained following nested PCR using first primers #1 and #26 and then primers #2 and #21 (see Experimental Procedures). The arrow marks 104 bp, the predicted size of products following the second amplification; the left-most lane contains molecular weight standards obtained from an MspI digest of pBR322. Amplification products of the predicted size were obtained using genomic DNA from the C27-3 cell line (lane 1) but not from C17-2 (lane 2) or C36-4 (not shown). Cerebellar tissue from two C27-3 transplant recipients containing blue cells (the animal in Figures 1F and 1G, lanes 3–6, and the animal in Figures 2E and 2F, lanes 7–10) also yielded amplification products of the predicted size, identical to that from the C27-3 cell line (lane 1). Lanes that contained tissue from an uninjected cerebellum demonstrated no amplification product (lanes 11–14). Blue cells from the animal in Figures 2A–2D yielded amplification products identical to those in lanes 3–10. Lanes that contained tissue from a littermate in which engraftment failed (i.e., no blue cells) demonstrated no amplification product (not shown). "Shadow bands" as seen in the lane with genomic DNA from the C27-3 cell line (lane 1) do not appear when only 45 cycles of unnested PCR are performed with primers #2 and #21 alone (not shown).

Stanfield and O'Leary, 1985; O'Leary and Stanfield, 1989; Lund et al., 1987). Reconstitution of lost function has also been achieved through transplantation, using either primary fetal– or tumor-derived tissue (Barry et al., 1987; Isacson et al., 1986; Gage et al., 1983; Fisher et al., 1991; Bjorklund et al., 1982; Buzsaki et al., 1988; Rosenberg et al., 1988; Sotelo and Alvarado-Mallart, 1986, 1987; Labbe et al., 1983; O'Leary and Stanfield, 1989; Freund et al., 1985). The transplantation data presented in this article and in a recent report by Renfranz et al. (1991) represent a demonstration of cytoarchitecturally and, perhaps, functionally appropriate engraftment by exogenous mammalian central neural tissue that is neither tumorigenic nor of tumor or primary fetal origin. The potential would seem to exist for transplanting such lines for repair in lesioned or mutant animals or for the transport of genes of developmental or therapeutic interest into the CNS. Furthermore, the techniques for generating transplant material in this manner may conceivably someday circumvent concerns over the use of primary fetal tissue. However, since problems with efficiency of stable engraftment remain poorly understood and thus difficult to control, much work remains prior to the use of such lines for clinical applications.

Resemblance to Endogenous Cerebellar Progenitors

Following the progeny derived from a single progenitor maintained in culture has been useful for defining a range of potentials for a subset of neuroblasts (Baroffio et al., 1988; Temple, 1989). Immortalization and cloning of individual progenitors represents another approach to the question of potency. While both approaches suffer from inherent limitations, such as removal of a cell from its in vivo context, it was hoped that the availability of an unlimited number of cells derived from a single progenitor would offer some advantages over primary cultures. One hope was that the act of immortalization would freeze a progenitor cell in a particular state, providing a source of homogeneous cells that could be manipulated to alter the fate of its progeny. However, in this case, as in many others in which CNS cells were immortalized, homogeneity has been observed only rarely (Ryder et al., 1990; Cepko, 1988; Evrard et al., 1990; Fredericksen et al., 1988; Bartlett et al., 1988; Birren and Anderson, 1990; Geller and Dubois-Dalcq, 1988). Instead, immortalization of single progenitors yields clonal lines that are both heterogeneous and plastic (i.e., changing over time in culture). Subsets of the same line often express both neuronal and glial phenotypes concurrently and/or alternate "spontaneously" between the two. It is unclear whether these observations are the result of a self-renewing "pool" of uncommitted precursors responding specifically to changing signals or of stochastic changes, perhaps including transdifferentiation.

To determine whether lines are bona fide representatives of endogenous cells or are simply an artifact, one can compare their behavior to that of their counterparts left in situ. In situ lineage mapping using retroviral vectors and injection of tracers has allowed an examination of the potency of individual progenitors of the vertebrate CNS. In the retina (Turner and Cepko, 1987; Turner et al., 1990; Holt et al., 1988; Wetts and Fraser, 1988), tectum (Gray et al., 1988; Galileo et al., 1990), and spinal cord (Leber et al., 1990), individual endogenous neural progenitors were found to give rise to multiple neural cell types of both neuronal and glial phenotype. This assessment was enabled by the fact that clonally derived cells in these regions remained as identifiable clusters into adulthood. The ability to extend this technique and its conclusions, however, to mammalian CNS as a whole has been confounded by the observation of extensive migration of clonally related cells in several other regions, including cortex (Walsh and Cepko, 1988; Austin and Cepko, 1990), striatum (Halliday and Cepko, unpublished data), and, as illustrated here, cerebellum. Thus, currently there are no interpretable data on the potency of an individual EGL cell in situ, although efforts are underway in our laboratory to solve these problems (E. F. Ryder and C. L. Cepko, unpublished data).

However, one can use other methods to assess how closely immortalized cerebellar cells resemble primary

cells in culture and/or differentiated cerebellar cells in situ. C27-3, for example, exhibits a number of cerebellar antigens. C17-2, cocultured with primary astrocytes or with the U251 human astrocytoma cell line, has the ability to inhibit proliferation and induce differentiation of these cells (Weinstein et al., 1990), as has been described for cultured primary GCs (Hatten et al., 1986). Both C17-2 and C27-3 induce neurite outgrowth in cultured primary cerebellar neurons (J. R. Madsen, unpublished data). Finally, the lines express other cerebellar-specific proteins. En-1 and En-2 constitute a murine homeodomain family homologous to Drosophila *engrailed*. En-1 has been localized throughout the neuraxis in developing embryos; En-2 is restricted to a subset of En-1$^+$ cells specifically in the hindbrain of the embryo and, ultimately, the IGL of adult cerebellum (Davis et al., 1988; Davidson et al., 1988; Joyner et al., 1991). The lines express these proteins to various degrees (A. Joyner, personal communication). All of these features suggest that these lines at least resemble primary cerebellar tissue.

An additional way to investigate the authenticity of the lines, however, is to demonstrate incorporation of these cells into the cytoarchitecture of the appropriate brain region at the appropriate host age. When newborn mouse cerebella were transplanted with cell lines, it was seen that transplanted cells derived originally from the EGL had reincorporated into the EGL. At adulthood, cells of these lines were observed to have differentiated into multiple cell types classically thought to be derived from the EGL (Miale and Sidman, 1961; Palay and Chan-Palay, 1974; Altman, 1982), including GC and BC neurons as well as glia (oligodendrocytes and astrocytes). However, since a recent report (Hallonet et al., 1990) has called into question the classical view of the EGL progenitor–progeny relationships, it is difficult to interpret whether the cell types recovered after transplantation offer evidence of an EGL cell line or of a cerebellar or CNS progenitor with broader potential.

Comparison with Mature, Endogenous Cerebellar Cells

Although engrafted cells in the first week resemble endogenous EGL cells, at adulthood, many transplant-derived GCs appear "plumper" at the light microscopic level than their endogenous GC counterparts labeled directly with the BAG virus (e.g., Figures 3A and 3B). Processes and cytoplasm of transplanted cells appear more "distended" with precipitate. We cannot explain this difference in labeling pattern. At the EM level, however, transplant-derived cells resembled their endogenous unlabeled cell-type counterparts, indicating that they had differentiated into GC and BC neurons and glia. The value of the transplanted lines for addressing developmental and/or clinical issues hinges on their functional fidelity to endogenous neural cells. EM analysis provided evidence that some transplanted cells that differentiated into ultrastructurally identifiable GC neurons developed dendrites that were postsynaptic to the appropriate presynaptic areas on mossy fibers (Figure 6), suggesting functional as well as anatomic integration. This is based on the observation that some dendrites contained the characteristic X-gal precipitate. The X-gal reaction product could theoretically have diffused from donor cell bodies onto dendrites of host cells. However, the fact that the precipitate was usually membrane bound within cell bodies, respected dendritic membranes, and was not seen in inappropriate locations (e.g., the presynaptic mossy fibers) would seem to argue against this potential problem. Additional observations of a greater number of animals that bear large numbers of engrafted cells and thus allow EM analysis of synaptic structures is required to confirm and extend these findings.

The Engraftment Process

We cannot yet distinguish among several scenarios regarding the nature of the cells that actually engraft. For example, engraftment by mitotic, uncommitted progenitors may produce progeny that differentiate in response to position-dependent microenvironmental cues. Alternatively, committed mitotic progenitors may engraft and produce progeny that differentiate following migration. Engraftment may also occur by differentiated postmitotic cells that migrate to their appropriate loci, or there may be a selection by the microenvironment among many postmitotic cells that randomly distribute. Our analyses of animals shortly following transplantation suggest that a scenario in which postmitotic cells are the only cells that engraft is rather unlikely. When the animals were examined within a few days of transplantation, a relatively small number of cells actually seemed to appose the EGL. Furthermore, a small percentage of the inoculum actually integrated and appeared to migrate. In situations in which large numbers of transplanted cells were ultimately seen at adulthood, we favor the hypothesis that mitotic cells, rather than many postmitotic cells, engrafted, replicated, and differentiated in response to particular microenvironmental cues. However, because injections may vary from animal to animal, it is possible that animals with large numbers of engrafted cells, by chance, received an inoculum that was in some way more efficient with respect to placement and/or survival of postmitotic cells. Furthermore, there is some indication that even cells that express differentiation-specific markers, including NF, may continue to divide (Ryder et al., 1990). As efficiency and uniformity of transplantation increase, these possibilities may be better distinguished by paired experiments wherein markers or inhibitors of mitotic activity are administered to cultures prior to transplantation and the number and phenotype of successfully engrafted cells are compared.

Ruling Out Viral Contamination

That staining at the microscopic level of transplant-derived cells, as well as their distribution, differs from that of cells labeled directly by injected virus actually provides some evidence that blue cells in transplant recipient brains are not due to viral contamination. Further reassurance was the demonstration that the viral insertion site in the donor cell line was identical to that in blue cells recovered from the engrafted animals. In addition, multiple tests for production of BAG virus by C27 and C17 were run and found to be uniformly negative.

Long-Term Expression of an Exogenous Gene

Implicit in these studies is evidence for successful expression of an exogenous gene (*lacZ*) following incorporation of transplanted neural tissue. In some cases, expression could be demonstrated after 22 months (e.g., Figures 1F and 1G; Figures 4–6). While histochemistry allows us to infer positive expression in blue cells, we cannot rule out the possibility that some "white" cells are also transplant derived but fail to express the *lacZ* gene at levels detectable using the X-gal histochemistry. White cells appear within dishes of clonal *lacZ*$^+$ cells spontaneously over time in the culture and appear to correlate with lack of expression from the viral LTR (S. Fields-Berry and C. L. Cepko, unpublished data). One interpretation of the higher apparent engraftment rate after short survival (56%) vs. long survival (8%) is that inactivation of β-galactosidase expression occurs at a significant frequency over time. Of course, alternative explanations, such as cell death, may also pertain. The availability of a genetic tag detectable by PCR will allow for an independent test of whether the cells are indeed present, but undetectable by X-gal histochemistry. The recent availability of an alternative marker gene that shows less loss of expression in culture may also circumvent the problem (e.g., alkaline phosphatase [Fields-Berry et al., 1992]).

myc Expression in the Cerebellum

The proto-oncogene c-*myc* is expressed in mouse cerebellar neurons at different levels during different developmental stages (Ruppert et al., 1986). It appears that progenitor cells accumulate c-*myc* message during proliferation and/or in preparation for differentiation. Down-regulation of *myc* expression is correlated with differentiation (Griep and Westphal, 1988; Morse et al., 1986). While it is obvious that tumors do not form, we do not know whether v-*myc* continues to be expressed following transplantation and differentiation of C27-3 or C17-2. However, studies in other systems (La Rocca et al., 1989; Palmieri et al., 1983) indicate that interaction of v-*myc*-transformed cells with normal cells in mixed cultures suppresses the transformed phenotype. In these cases, proliferation is suppressed and reexpression of the differentiated cellular program occurs, even without down-regulation of v-*myc* expression. Our experiments wherein cerebellar cell lines were cocultured with primary cerebellar cells seem to reproduce this phenomenon. The same phenomenon may occur in vivo following transplantation. Future studies will seek to determine the extent of v-*myc* expression in engrafted cells.

Future Directions

The potential of C27-3 and C17-2 can be further explored using a variety of transplantation recipients and protocols. The availability of murine mutants with specific cell-type deficiencies in the cerebellum will allow an additional test of the competence, potential, and fidelity of these lines via complementation experiments. Since the present studies did not examine whether these cells are committed or restricted to cerebellar fate, examination of engraftment of lines in regions and at developmental periods other than those from which they were generated are being carried out to allow an assessment of this property. Preliminary evidence indicates that these lines may engraft in regions of the CNS outside the cerebellum (E. Y. Snyder, S. A. Arnold, and C. L. Cepko, unpublished data). Whether genes of reportedly site-specific expression are expressed by these lines in new locations might help to test hypotheses that hold that specification of the spatial domains of different cell populations during CNS development proceeds by the progressive expression or loss of expression of various regulatory genes. Availability of engraftable lines that can be stably transduced with exogenous genes and presumably manipulated by homologous recombination techniques to achieve other alterations of regulatory genes may facilitate functional tests of these regulatory events.

Experimental Procedures

Propagation of Cerebellar Cell Lines

Cerebellar cell lines were generated as previously described (Ryder et al., 1990). Lines were grown in Dulbecco's modified Eagle's medium supplemented with 10% fetal calf serum (Gibco), 5% horse serum (Gibco), and 2 mM glutamine on poly-L-lysine (PLL) (Sigma) (10 μg/ml)–coated tissue culture dishes (Corning). (While the lines grew well on uncoated tissue culture dishes, the most successful differentiation and subsequent engraftment may be associated with prior plating on a PLL substrate.) The lines were maintained in a standard humidified, 37°C, 5% CO_2–air incubator and were either fed weekly with one-half conditioned medium from confluent cultures and one-half fresh medium or split (1:10 or 1:20) weekly or semiweekly into fresh medium. Changes in brand of tissue culture plastic, type of substrate coat, and type and concentration of serum might change the phenotypes displayed by the lines. Lines appeared to engraft most successfully when, prior to transplantation, they: were in an active growth phase; yielded process-bearing cells; displayed immunocytochemical neural cell type–specific markers (e.g., NF and/or GFAP); and, for purposes of detection, when they had >50% of their cells positive with X-gal.

Immunocytochemistry

The markers routinely chosen were those that have been well-associated with differentiated neurons—NF (Wood and Anderton, 1981; monoclonal antibody 8A1, courtesy of C. Barnstable)—and with differentiated glial cells—galactocerebroside C for oligodendrocytes (Raff et al., 1978; hybridoma supernatant courtesy of B. Ranscht) and GFAP for astrocytes (Bignami et al., 1972; monoclonal antibody from Boehringer). Dilutions of NF (1:100) and GFAP (1:4) were in Dulbecco's modified Eagle's medium supplemented with 10% goat serum, 0.3% Triton X-100, and 0.05% azide; anti–galactocerebroside C hybridoma supernatant was used undiluted. The secondary antibody was fluorescein- or biotin-conjugated goat α-mouse. A monoclonal antibody directed against an irrelevant antigen served as a negative control for nonspecific staining. Immunofluorescence methodology was outlined in Ryder et al. (1990). When immunoperoxidase or immunoalkaline phosphatase staining was desired, the ABC kit and procedures from Vector Laboratories were used (Fields-Berry et al., 1992). For staining of tissue sections, tissue was first dehydrated through graded alcohols and xylenes, embedded in paraffin at 60°C, sliced into 1 μm sections on a Reichert-Jung Biocut microtome, transferred to heated (60°C) 1%–3% gelatin-coated slides, deparaffinized and rehydrated through reverse-graded xylenes and alcohols, and stained for immunocytochemistry as for cultured cells using the immunoperoxidase or immunoalkaline phosphatase method. If double labeling of X-gal$^+$ cells and cell type–specific markers was desired, the X-gal reaction was performed first on gluteraldehyde-fixed tissue, prior to embedding in paraffin. To examine isolated, individual cells from a 1 μm tissue section that had been analyzed immunohistochemically, the section was mechanically dissociated by "squashing," i.e., placing gentle but firm,

concentrated pressure on the portion of coverslip overlying the section, in planes both perpendicular and parallel to the section.

Transduction of Cerebellar Progenitor Lines with *lacZ* Gene

A recent 1:10 split of the cell line of interest was plated onto 60 mm tissue culture plates. Between 24 and 48 hr after plating, the cells were incubated with the replication-incompetent retroviral vector BAG (10^6–10^7 colony-forming units [cfu]/ml) plus 8 μg/ml polybrene for 1–4 hr. Cells were then cultured in fresh feeding medium for approximately 3 days until they appeared to have undergone at least two doublings. The cultures were then trypsinized and seeded at low density (50–5000 cells on a 100 mm tissue culture dish). After approximately 2 weeks, well-separated colonies were isolated by brief exposure to trypsin within plastic cloning cylinders. Colonies were plated in 24-well PLL-coated CoStar plates. At confluence, these cultures were passaged to 60 mm tissue culture dishes and expanded. A representative dish from each subclone was stained directly in the culture dish using X-gal histochemistry (see Price et al., 1987; Cepko, 1989a, 1989b). The percentage of blue cells was counted under the microscope. Subclones with the highest percentage of blue cells (ideally >90%; at least >50%) were maintained, characterized, and used for transplantation.

Tests for Virus Transmission

The presence of helper virus was assayed by measurement of reverse transcriptase activity in supernatants of cell lines as described by Goff et al. (1981) and by testing the ability of supernatants to infect NIH 3T3 cells and generate G418-resistant colonies or X-gal$^+$ colonies (detailed in Cepko, 1989a, 1989b). All cerebellar cell lines used for transplantation were helper virus–free as judged by these methods.

Coculture of Neural Cell Lines with Primary Cerebellar Tissue

Primary dissociated cultures of neonatal mouse cerebellum were prepared as in Ryder et al. (1990) and seeded at a density of 2×10^5 to 4×10^5 cells per PLL-coated eight-chamber LabTek glass or plastic slide (Miles). After the cells settled (usually 24 hr), 10% of a nearly confluent 10 cm dish of the neural cell line of interest was seeded, following trypsinization, onto the slide. The coculture was re-fed every other day and grown in a 5% CO_2–air, humified incubator until 8 or 14 days of coculture. It was then fixed and processed for X-gal histochemistry (detailed in Price et al., 1987; Cepko, 1989a, 1989b).

Preparation of Cell Lines for Transplantation

Cells from a nearly confluent but still actively growing dish of donor cells were washed twice with phosphate-buffered saline (PBS), trypsinized, gently triturated with a wide-bore pipette in serum-containing medium (to inactivate the trypsin), gently pelleted (1100 rpm for 1 min in a clinical centrifuge), and resuspended in 5 ml of PBS. Washing by pelleting and resuspension in fresh PBS was repeated twice, with the cells finally resuspended in a reduced volume of PBS to yield a high cellular concentration (at least 1×10^4 cells per μl). Trypan blue (0.05% [w/v]) was added to localize the inoculum. The suspension was kept well triturated, albeit gently, and maintained on ice prior to transplantation to minimize clumping.

Injections into Postnatal Cerebellum

Newborn CD-1 or CF-1 mice were cryoanesthetized, and the cerebellum was localized by transillumination of the head. Cells were administered either via a Hamilton 10 μl syringe with a beveled 33-gauge needle or a drawn glass micropipette with a 0.75 mm inner diameter and 1.0 mm outer diameter generated from borosilicate capillary tubing (FHC, Brunswick, ME) by a Flaming Brown Micropipette Puller (Model p-87, Sutter Instruments) using the following parameters: heat 750, pull 0, velocity 60, time 0. Best results were achieved with the glass micropipette. The tip was inserted through the skin and skull into each hemisphere and vermis of the cerebellum where the cellular suspension was injected (usually 1–2 μl per injection). Typically, the following situation existed: 1×10^7 cells per ml of suspension; 1×10^4 to 2×10^4 cells per injection; one injection in each cerebellar hemisphere and in the vermis. Importantly, the cellular suspension, maintained on ice throughout, was gently triturated prior to each injection in order to diminish clumping and to keep cells suspended.

The injection of BAG virus was performed as described for the cell suspension. The BAG virus stock (8×10^7 G418-resistant cfu/ml) contained, in addition to trypan blue, polybrene at 8 μg/ml.

Processing of Tissue for β-Galactosidase Histochemical Detection by Light Microscopy

Mice were killed by barbituate or ketamine overdose and perfused first with 10 ml of PBS (pH 7.3), $MgCl_2$ (2 mM), EGTA (2 mM) followed by 30 ml of 2% paraformaldehyde in 0.1 M PIPES buffer (pH 6.9), $MgCl_2$ (2 mM), EGTA (2 mM) for over 30 min. β-Galactosidase activity was detected by incubation of the tissue in 5-bromo-4-chloro-3-indoyl β-D-galactoside (X-gal) as detailed in Cepko (1989a, 1989b). Cellular location and morphology in tissue sections were enhanced as needed with Nomarski optics permitting reliable cell-type identification within cerebellum (Palay and Chan-Palay, 1974).

Electron Microscopy of Tissue Reacted for X-Gal Histochemistry

Processing of tissue for X-gal histochemistry was as previously described (Cepko, 1989a, 1989b), except that all fixation of experimental tissue, including the fix for perfusion of animals, was performed with a modified Karnovsky's Fixative (2% paraformaldehyde, 2.5% glutaraldehyde, 4.1% sucrose in PIPES) without the addition of detergents but with $MgCl_2$ (2 mM) and EGTA (2 mM). Rather than embedding frozen tissue in OCT embedding compound for cryostat sectioning, the tissue was sliced into 100 μm coronal sections using a McIlwain tissue chopper (Brinkman) or into 0.2–0.5 mm parasagittal sections under a dissecting scope using razor blades. These tissue slices were processed as floating sections using X-gal histochemistry. It was possible, under these conditions, to obtain adequate staining of labeled cells with no background if embedded as soon as possible (within 3 days). The cells were located under a dissecting scope (50×), and the appropriate tissue slice was selected for further processing for electron microscopy, using standard techniques. Briefly, the tissue was reacted with 1% osmium tetroxide in PBS (w/v), washed well in PBS followed by distilled water, stained en bloc in 1% uranyl acetate in distilled water (w/v), dehydrated through graded alchohols, exposed for 10 min to propylene oxide and to propylene oxide plus accelerated (DMP-30) epon–araldite (1:1) for a length of time from 15 min to overnight (shorter times optimal), and embedded in accelerated epon–araldite from which ultrathin sections were cut and transferred to Formvar-coated slot grids. (Multiple absolute ethanol washes was an alternative dehydration technique.) The grids were not further reacted with lead citrate or uranyl acetate. They were observed on a Joel 1000C electron microscope, and photomicrographs were taken at 60 kv and spot size 1 with the smallest objective aperture. The X-gal reaction product (a 5-bromo-4-chloro-3-indoyl precipitate) examined in this fashion was electron dense, allowing identification of transplanted cells (Bonnerot et al., 1987). Cells were evaluated only if they contained label that was confined to subcellular organelles and/or respected membranes. Excellent fixation is required to identify postsynaptic specializations on GC dendrites. One of the 4 positive animals examined ultrastructurally (Table 1) met this criterion, permitting the successful identification of synapses. Fixation in the remaining 3 animals was inadequate to assess the presence or absence of synapses. To measure the width of such intermediate filaments as GFs and NFs, fibers were magnified to the equivalent of 74,000×, printed on photographic paper, and measured directly. As an internal control for calibration error within the microscope, the populations of GFs and NFs measured were from the same negative. The average width of GFs was 8.4 nm (expected: 8–9 nm); the average width of NFs was 11.1 nm (expected: 10–12 nm), values acceptable within the 10%–20% calibration error of the microscope. The width ratio of GFs to NFs was within the expected 70%–80% range, verifying internal consistency.

Determination of Integration Site in Engrafted Cells by the PCR

Genomic DNA from the cell line C27-3 was prepared by standard techniques (Maniatis et al., 1982). Because the integrated proviral LTR contained no recognition sites for TaqI, digestion with TaqI endonuclease yielded fragments that included the LTR and unique portions of the host flanking sequences. DNA fragments were then ligated into circles using T4 DNA ligase (New England BioLabs) at a final DNA concentration of 1 ng/μl in ligation buffer. The DNA (10 ng) was then

amplified by an "inverse PCR" (Ochman et al., 1988): the ligated DNA circles were relinearized by digestion with XbaI (New England BioLabs), which cuts once in the LTR, and the fragments were then amplified using two oppositely oriented oligonucleotide primers within the LTR on opposite sides of the XbaI site (primer #21: TCTCCTCTGAGTGATTGACTACCCGTCAGC; primer #22: TGATCTGAACTTCTCTCTATTCTCAGTTATGT). The amplified fragment was sequenced following introduction into the Mp18 site of an M13 cloning vector (Pharmacia), and the flanking sequences were identified. Two oligonucleotides of 27 bp, complementary to portions of this now known flanking sequence and progressively closer to the LTR, were synthesized on an Applied Biosystems Oligonucleotide Synthesizer (primer #1: GGCACTAACTTTTCTTCCTCCCAGTGG; primer #2: GAGCAGGTGCAGGATTCTGATTTCACG). These served as one-half of a set primers for subsequent direct nested PCR against opposing primers within the LTR (primer #21: sequence as above; primer #26: AGTTGCATCCGACTTGTGGTCTCGCTGTTC).

After histochemical processing of a transplant recipient's cerebellum for X-gal$^+$ cells, small pieces of tissue, each containing 1–20 blue cells, were dissected from various regions and transferred to separate wells of a Falcon Microtest III Flexible Assay Plate, containing 10 μl of a mixture of 200 μg/ml proteinase K, 0.5% Tween 20, 1.5 mM $MgCl_2$, 50 mM KCl, and 10 mM Tris buffer (pH 8.3). After incubation at 65°C for 30 min, the protease was inactivated at 85°C for 20 min. The following were then added: PCR buffer (1.2 mM $MgCl_2$, 10 mM Tris buffer (pH 8.3), 50 mM KCl), deoxyribonucleotides (final concentration, 200 μm each), 0.5 U of Taq DNA polymerase (Cetus), and 1 μM each of a pair of oppositely oriented oligonucleotide primers (one in the flanking region [primer #1], the other within the LTR [primer #26]). Following 45 cycles of PCR amplification (1 cycle consisted of 94°C for 45 s, 60°C for 45 s, and 72°C for 2 min), a 5 μl aliquot from each of the first reaction products was used in a second PCR amplification (25–35 cycles) employing a second set of oligonucleotides internal to the first (a "nested amplification") (primer #2 and primer #21) (Mullis and Faloona, 1989). Samples of genomic DNA from the cell line served as positive controls. Cerebella from littermates in which engraftment failed (no blue cells), uninjected cerebella, and samples containing no tissue served as negative controls. At least 10 μl of amplified product from the second amplification was electrophoresed on a 3% NuSieve–1% SeaKem agarose gel plus 1 μg/ml ethidium bromide with Tris–acetate–EDTA or Tris–borate–EDTA buffer (as per Maniatis et al., 1982). Bands of the appropriate size were identified using ethidium bromide staining.

Acknowledgments

This work was supported in part by grants to E. Y. S. from the National Institute of Neurological Disorders and Stroke (Clinical Investigator Development Award 5-K08-NS01403-02) and from the William Randolph Hearst Foundation. Support also came from the Searle Scholars Program to C. L. C. and the Dana Foundation to C. W.

We thank Drs. Elizabeth Hay at Harvard Medical School and Marian DiFiglia at the Neuroscience Center at Massachusetts General Hospital who kindly made available their EM facilities. We are deeply indebted to Dr. Sanford L. Palay for generously sharing with us his expertise in the ultrastructure of the cerebellum, helping us to evaluate our EM material, and aiding us in the identification of cerebellar structures. We are also grateful to Dr. Elio Raviola for invaluable advice on the preparation and assessment of our material.

The costs of publication of this article were defrayed in part by the payment of page charges. This article must therefore be hereby marked "*advertisement*" in accordance with 18 USC Section 1734 solely to indicate this fact.

Received June 27, 1991; revised October 23, 1991.

References

Altman, J. (1982). Morphological development of the rat cerebellum and some of its mechanisms. In The Cerebellum: New Vistas, S. L. Palay and V. Chan-Palay, eds. (Heidelberg: Springer-Verlag), pp. 8–49.

Austin, C. P., and Cepko, C. L. (1990). Cellular migration patterns in the developing mouse cerebral cortex. Development *110*, 713–732.

Baroffio, A., Dupin, E., and Le Douarin, N. M. (1988). Clone-forming ability and differentiation potential of migratory neural crest cells. Proc. Natl. Acad. Sci. USA *85*, 5325–5329.

Barry, D. I., Kikvadze, I., Brundin, P., Bolwig, T. G., Bjorklund, A., and Lindvall, O. (1987). Grafted noradrenergic neurons suppress seizure development in kindling-induced epilepsy. Proc. Natl. Acad. Sci. USA *84*, 8712–8715.

Bartlett, P. F., Reid, H. H., Bailey, K. A., and Bernard, O. (1988). Immortalization of mouse neural precursor cells by the *c-myc* oncogene. Proc. Natl. Acad. Sci. USA *85*, 3255–3259.

Bignami, A., Eng, L. F., Dahl, D., and Uyeda, C. T. (1972). Localization of the glial fibrillary acidic protein in astrocytes by immunofluorescence. Brain Res. *43*, 429–435.

Birren, S. J., and Anderson, D. J. (1990). A v-*myc*-immortalized sympathoadrenal progenitor cell line in which neuronal differentiation is initiated by FGF but not NGF. Neuron *4*, 189–201.

Bjorklund, A., Stenevi, U., Dunnett, S. B., and Gage, F. H. (1982). Cross-species neural grafting in a rat model of Parkinson's disease. Nature *298*, 652–654.

Bonnerot, C., Rocancourt, D., Briand, P., Grimber, G., and Nicolas, J.-F. (1987). A β-galactosidase hybrid protein targeted to nuclei as a marker for developmental studies. Proc. Natl. Acad. Sci. USA *84*, 6795–6799.

Buzsaki, G., Ponomareff, G., Bayardo, F., Shaw, T., and Gage, F. H. (1988). Suppression and induction of epileptic activity by neuronal grafts. Proc. Natl. Acad. Sci. USA *85*, 9327–9330.

Cepko, C. L. (1988). Retrovirus vectors and their applications in neurobiology. Neuron *1*, 345–353.

Cepko, C. L. (1989a). Retrovirus-mediated immortalization of neural cells. Annu. Rev. Neurosci. *12*, 47–65.

Cepko, C. L. (1989b). Lineage analysis and immortalization of neural cells via retrovirus vectors. In Neuromethods, vol. 16, Molecular Neurobiological Techniques, A. A. Boulton, G. B. Baker, and A. T. Campagnoni, eds. (Clifton, New Jersey: Humana Press), pp. 177–219.

Davidson, D., Graham, E., Sime, C., and Hill, R. (1988). A gene with sequence similarity to Drosophila *engrailed* is expressed during the development of the neural tube and vertebrae in the mouse. Development *104*, 305–316.

Davis, C. A., Noble-Topham, S. E., Rossant, J., and Joyner, A. L. (1988). Expression of the homeobox-containing gene *En-2* delineates a specific region of the developing mouse brain. Genes Dev. *2*, 361–371.

Eccles, J. C., Ito, M., and Szentagothai, J. (1967). The Cerebellum As a Neuronal Machine (New York: Springer-Verlag).

Evrard, C., Borde, I., Marin, P., Galiana, B. E., Premont, J., Gros, F., and Rouget, P. (1990). Immortalization of bipotential and plastic glio-neuronal precursor cells. Proc. Natl. Acad. Sci. USA *87*, 3062–3066.

Fields-Berry, S. C., Halliday, A. L., and Cepko, C. L. (1992). Novel recombinant retrovirus encoding alkaline phosphatase confirms clonal boundary assignment in lineage analysis of murine retina. Proc. Natl. Acad. Sci. USA, in press.

Fisher, L. J., Jinnah, H. A., Kale, L. C., Higgins, G. A., and Gage, F. H. (1991). Survival and function of intrastriatally grafted primary fibroblasts genetically modified to produce L-dopa. Neuron *6*, 371–380.

Fredericksen, K., Jat, P. S., Valtz, N., Levy, D., and McKay, R. (1988). Immortalization of precursor cells from the mammalian CNS. Neuron *1*, 439–448.

Freund, T. F., Bolam, J. P., Bjorklund, A., Stenevi, U., Dunnett, S. B., Powell, J. F., and Smith, A. D. (1985). Efferent synaptic connections of grafted dopaminergic neurons reinnervating the host neostriatum: a tyrosine hydroxylase immunocytochemical study. J. Neurosci. *5*, 603–616.

Gage, F. H., and Fisher, L. J. (1991). Intracerebral grafting: a tool for the neurobiologist. Neuron *6*, 1–12.

Gage, F. H., Dunnett, S. B., Stenevi, U., and Bjorklund, A. (1983). Aged rats: recovery of motor impairments by intrastriatal nigral grafts. Science *221*, 966–968.

Galileo, D. S., Gray, G. E., Owens, G. C., Majors, J., and Sanes, J. R. (1990). Neurons and glia arise from a common progenitor in chicken optic tectum: demonstration with two retroviruses and cell-type specific antibodies. Proc. Natl. Acad. Sci. USA *87*, 458–462.

Geller, H. M., and Dubois-Dalcq, M. (1988). Antigenic and functional characterization of a rat central nervous system–derived cell line immortalized by a retroviral vector. J. Cell Biol. *107*, 1977–1986.

Goff, S., Traktman, P., and Baltimore, D. (1981). Isolation and properties of Moloney murine leukemia virus mutants: use of a rapid assay for release of virion reverse transcriptase. J. Virol. *38*, 239–248.

Gravel, C., Leclerc, N., Rafrafi, J., Sasseville, R., Thivierge, L., and Hawkes, R. J. (1987). Monoclonal antibodies reveal the global organization of the cerebellar cortex. J. Neurosci. Meth. *21*, 145–157.

Gray, G. E., Glover, J. C., Majors, J., and Sanes, J. R. (1988). Radial arrangement of clonally related cells in the chicken optic tectum: lineage analysis with a recombinant retrovirus. Proc. Natl. Acad. Sci. USA *85*, 7356–7360.

Griep, A. E., and Westphal, H. (1988). Antisense *myc* sequences induce differentiation of F9 cells. Proc. Natl. Acad. Sci. USA *85*, 6806–6810.

Hallonet, M. E. R., Treillet, M.-A., and Le Douarin, N. M. (1990). A new approach to the development of the cerebellum provided by the quail-chick marker system. Development *108*, 19–31.

Hatten, M. E., Liem, R. K. H., and Mason, C. A. (1986). Weaver mouse cerebellar granule neurons fail to migrate on wild-type astroglial processes in vitro. J. Neurosci. *6*, 2676–2683.

Holt, C. E., Bertsch, T. W., Ellis, H. M., and Harris, W. A. (1988). Cellular determination in the Xenopus retina is independent of lineage and birth date. Neuron *1*, 15–26.

Isacson, O., Dunnett, S. B., and Bjorklund, A. (1986). Graft-induced behavioral recovery in an animal model of Huntington disease. Proc. Natl. Acad. Sci. USA *83*, 2728–2732.

Joyner, A. L., Herrup, K., Auerbach, B. A., Davis, C. A., and Rossant, J. (1991). Subtle cerebellar phenotype in mice homozygous for a targeted deletion of the *En-2* homeobox. Science *251*, 1239–1243.

Labbe, R., Firl, A., Mufson, E. J., and Stein, D. G. (1983). Fetal brain transplants: reduction of cognitive deficits in rats with frontal cortex lesions. Science *221*, 470–472.

La Rocca, S. A., Grossi, M., Falcone, G., Alemà, S., and Tatò, F. (1989). Interaction with normal cells suppresses the transformed phenotype of v-*myc*-transformed quail muscle cells. Cell *58*, 123–131.

Leber, S. M., Breedlove, S. M., and Sanes, J. R. (1990). Lineage, arrangement, and death of clonally related motoneurons in chick spinal cord. J. Neurosci. *10*, 2451–2462.

Lund, R. D., Rao, K., Hankin, M. H., Kunz, H. W., and Gill, T. J., III (1987). Transplantation of retina and visual cortex to rat brains of different ages. Maturation, connection patterns, and immunological consequences. Ann. NY Acad. Sci. *495*, 227–241.

Maniatis, T., Fritsch, E. F., and Sambrook, J. (1982). Molecular Cloning: A Laboratory Manual (Cold Spring Harbor, New York: Cold Spring Harbor Laboratory).

McConnell, S. K. (1985). Migration and differentiation of cerebral cortical neurons after transplantation into the brains of ferrets. Science *229*, 1268–1271.

McConnell, S. K. (1988). Fates of visual cortical neurons in the ferret after isochronic and heterochronic transplantation. J. Neurosci. *8*, 945–974.

Miale, I., and Sidman, R. L. (1961). An autoradiographic analysis of histogenesis in the mouse cerebellum. Exp. Neurol. *4*, 277–296.

Morse, H. C., Hartley, J. W., Fredrickson, T. N., Yetter, R. A., Majumdar, C., Cleveland, J. L., and Rapp, U. R. (1986). Recombinant murine retroviruses containing avian v-*myc* induce a wide spectrum of neoplasms in newborn mice. Proc. Natl. Acad. Sci. USA *83*, 6868–6872.

Mullis, K. B., and Faloona, F. A. (1989). Specific synthesis of DNA in vitro via a polymerase catalyzed chain reaction. Meth. Enzymol. *155*, 335–350.

Ochman, H., Gerber, A. S., and Hartl, D. L. (1988). Genetic applications of an inverse polymerase chain reaction. Genetics *120*, 621–623.

O'Leary, D. D. M., and Stanfield, B. B. (1989). Selective elimination of axons extended by developing cortical neurons is dependent on regional locale: experiments utilizing fetal cortical transplants. J. Neurosci. *9*, 2230–2246.

Palay, S. L., and Chan-Palay, V. (1974). Cerebellar Cortex, Cytology and Organization (Heidelberg: Springer-Verlag).

Palmieri, S., Kahn, P., and Graf, T. (1983). Quail embryo fibroblasts transformed by four v-*myc*-containing virus isolates show enhanced proliferation but are nontumorigenic. EMBO J. *2*, 2385–2389.

Peters, A., Palay, S. L., and Webster, H. D. (1991). The Fine Structure of the Nervous System, Neurons and Their Supporting Cells, third edition (Oxford: Oxford University Press).

Price, J., Turner, D. L., and Cepko, C. L. (1987). Lineage analysis in the vertebrate nervous system by retrovirus-mediated gene transfer. Proc. Natl. Acad. Sci. USA *84*, 156–160.

Raff, M. C., Mirsky, R., Fields, K. L., Lisak, R. P., Dorfman, S. H., Silberberg, D. H., Gregson, N. A., Leibowitz, S., and Kennedy, M. C. (1978). Galactocerebroside is a specific cell-surface antigenic marker for oligodendrocytes in culture. Nature *274*, 813–816.

Rakic, P. (1971). Neuron–glia relationship during granule cell migration in developing cerebellar cortex. A golgi and electron microscopic study in Macacus rhesus. J. Comp. Neurol. *141*, 283–312.

Renfranz, P. J., Cunningham, M. G., and McKay, R. D. G. (1991). Region-specific differentiation of the hippocampal stem cell line HiB5 upon implantation into the developing mammalian brain. Cell *66*, 713–729.

Rosenberg, M. B., Friedmann, T., Robertson, R. C., Tuszynski, M., Wolff, J. A., Breakefield, X. O., and Gage, F. H. (1988). Grafting genetically modified cells to the damaged brain: restorative effects of NGF expression. Science *242*, 1575–1578.

Ruppert, C., Goldowitz, D., and Wille, W. (1986). Proto-oncogene c-*myc* is expressed in cerebellar neurons at different developmental stages. EMBO J. *5*, 1897–1901.

Ryder, E. F., Snyder, E. Y., and Cepko, C. L. (1990). Establishment and characterization of multipotent neural cell lines using retrovirus vector-mediated oncogene transfer. J. Neurobiol. *21*, 356–375.

Schaper, A. (1897). The earliest differentiation in the central nervous system of vertebrates. Science *5*, 430–431.

Smeyne, R. J., and Goldowitz, D. (1989). Development and death of external granular layer cells in the weaver mouse cerebellum: a quantitative study. J. Neurosci. *9*, 1608–1620.

Sotelo, C., and Alvarado-Mallart, R. M. (1986). Growth and differentiation of cerebellar suspensions transplanted into the adult cerebellum of mice with heredodegenerative ataxia. Proc. Natl. Acad. Sci. USA *83*, 1135–1139.

Sotelo, C., and Alvarado-Mallart, R. M. (1987). Embryonic and adult neurons interact to allow Purkinje cell replacement in mutant cerebellum. Nature *327*, 421–423.

Stanfield, B. B., and O'Leary, D. D. M. (1985). Fetal occipital neurones transplanted to the rostral cortex can extend and maintain a pyramidal tract axon. Nature *313*, 135–137.

Temple, S. (1989). Division and differentiation of isolated CNS blast cells in microculture. Nature *340*, 471–473.

Turner, D. L., and Cepko, C. L. (1987). A common progenitor for neurons and glia persists in rat retina late in development. Nature *328*, 131–136.

Turner, D. L., Snyder, E. Y., and Cepko, C. L. (1990). Lineage-independent determination of cell type in the embryonic mouse retina. Neuron *4*, 833–845.

Walsh, C., and Cepko, C. L. (1988). Clonally-related cortical cells show several migration patterns. Science *241*, 1342–1345.

Weinstein, D. E., Shelanski, M. L., and Liem, R. K. (1990). C17, a retrovirally immortalized neuronal cell line, inhibits the proliferation of

astrocytes and astrocytoma cells by a contact-mediated mechanism. Glia *3*, 130–139.

Wetts, R., and Fraser, S. E. (1988). Multipotent precursors can give rise to all major cell types of the frog retina. Science *239*, 1142–1145.

Wood, J. N., and Anderton, B. H. (1981). Monoclonal antibodies to mammalian neurofilaments. Biosci. Rep. *1*, 263–268.

Note Added In Proof

Please direct inquiries to the present address of E. Y. Snyder: Harvard Medical School, c/o Children's Hospital, 300 Longwood Avenue, 248 Enders, Boston, Massachusetts 02115.